



UNIVERSITÀ POLITECNICA DELLE MARCHE
FACOLTÀ DI INGEGNERIA

Corso di Laurea in Ingegneria Edile-Architettura

**Vibration-based dynamic characterization and
model updating of the Civic Tower of Ostra, Italy**

**Identificazione dinamica e calibrazione del modello
numerico della Torre Civica di Ostra**

Relatore:

Prof. Stefano Lenci

Stefano Lenci

Tesi di Laurea di:

Francesca Turchetti

Francesca Turchetti

Correlatori:

Ing. Francesco Clementi

Francesco Clementi

Ing. Maria Giovanna Masciotta

Maria Giovanna Masciotta

A.A. 2018/2019

*to all those who supported me
and believed in me*

Ringraziamenti

Alla fine di questo percorso formativo, ricco di esperienze positive che mi hanno infuso determinazione e passione, vorrei ringraziare tutte quelle persone che mi hanno sostenuto, spronato e che hanno condiviso con me questa esperienza.

Inizio con il ringraziare i miei tutor accademici, il prof Stefano Lenci e il prof Francesco Clementi, che mi hanno seguito con costanza e professionalità e mi hanno trasmesso la passione per intraprendere questo mestiere. Grazie alla loro esperienza e conoscenza, sono cresciuta giorno dopo giorno e sono riuscita a portare a termine questo lavoro di tesi. Ringrazio la prof.ssa Maria Giovanna Masciotta, dell'università di Guimarães, per la disponibilità e l'impegno con cui ha seguito la mia tesi, per avermi sempre incoraggiato e per avermi dato la possibilità di studiare in una università straniera. I mesi trascorsi in Portogallo sono stati estremamente formativi e mi hanno permesso di crescere sia professionalmente che caratterialmente.

Ringrazio i miei genitori per avermi sempre sostenuto, spronato e tranquillizzato. Mia mamma per essere stata sempre presente e avermi incoraggiato dal primo all'ultimo esame, per gli abbracci ad ogni esame superato, mio padre per aver sempre creduto in me e per avermi fatto imboccare la via della ragionevolezza anche nei momenti di confusione. Ringrazio Agnese, quale sorella acquisita dalla scuola materna, per la sua capacità di dire sempre la cosa giusta al momento giusto, per avermi supportato per tutto il percorso di studi e per essermi stata sempre vicina anche se in un'altra città o all'estero.

Esprimo gratitudine alle mie amiche di sempre Teresa, Camilla, Beatrice con le quali ho coltivato sempre un sentimento genuino e puro e so che su di voi posso contare sempre anche se fisicamente lontane.

Ringrazio tutti i miei amici anconetani, in particolare Lucia, Veronica e Alessia, con i quali ormai ho un legame di sangue, per essermi stati sempre vicini e per tutti i bei momenti trascorsi insieme.

Ringrazio i compagni e amici di università, per aver condiviso con me le esperienze positive, le delusioni e i momenti felici; in particolare un ringraziamento a Veronica, Camilla, Giulia, Gloria e Raffaella per il lavoro di squadra durante l'esperienza universitaria.

Un ringraziamento anche alle mie amiche di palestra per avermi fatto divagare nei momenti più stressanti.

Infine ringrazio tutti i miei insegnanti, dalla materna all'università, perché è grazie a loro che ho scoperto le mie qualità e le mie aspirazioni, che mi hanno aiutato a farmi imboccare la strada giusta.

Vi ho nel cuore in questo giorno, uno dei più importanti della mia vita, anche se siete lontani fisicamente ma vicini mentalmente. Grazie a tutti con sincero affetto.

Abstract

Nowadays, the preservation of historic buildings is becoming increasingly important especially in a country like Italy that boasts an innumerable amount of heritage structures and that is subject to important earthquakes in most of its regions. Seismic protection and vulnerability reduction are key issues that increased the interest in structural health monitoring as a powerful tool to identify early-stage damage of structures. Monitoring is an effective alternative to direct interventions because of its reliability and non-destructiveness. Recently, engineering has developed vibration-based methods for damage detection that has been rapidly expanding over the last few years.

The present thesis illustrates the results of a monitoring campaign on a masonry bell tower in Ostra (AN). The city of Ostra is located in an area with high seismic risk and recently suffered the strong earthquakes of 2016 and 2017: it is therefore possible that the tower was damaged due to the quake.

The main aim is the determination of modal properties of this historical masonry construction using experimental and numerical studies. The ambient vibration survey allowed performing an experimental analysis, the results of which were used to tune a numerical model of the structure based on finite element analysis with solid elements. The calibration was carried out in different steps, changing some parameters such as the modulus of elasticity, in order to get an accurate numerical model that simulates the dynamic behaviour of the whole structure. Obtaining good consistency between the experimental and numerical analyses, the study revealed the actual dynamic properties of the tower.

From the analysis of the results achieved, it is possible to make considerations and draw conclusions about possible damages in the structure.

The data collection about the monitoring of ancient and historic structures can be extremely helpful in identifying damage and planning interventions and contributes to the protection and maintenance of cultural heritage.

Riassunto

La conservazione degli edifici storici sta diventando una questione sempre più importante soprattutto in un paese come l'Italia che vanta un patrimonio culturale vastissimo e che, allo stesso tempo, è soggetto a importanti terremoti nella maggior parte delle sue regioni che rischiano di compromettere l'integrità delle strutture più vulnerabili. La protezione sismica e la riduzione della vulnerabilità sono questioni chiave e questo ha aumentato l'interesse per il monitoraggio strutturale come strumento per identificare i danni alle strutture in fase iniziale. Il monitoraggio è un'alternativa efficace agli interventi diretti grazie alla sua affidabilità e non distruttività. Di recente, l'ingegneria ha sviluppato metodi basati sull'acquisizione delle vibrazioni ed accelerazioni della struttura per il rilevamento dei danni che si sono rapidamente sviluppati negli ultimi anni.

La presente tesi illustra i risultati di una campagna di monitoraggio che ha interessato la torre civica di Ostra (AN). La città di Ostra si trova in una zona ad alto rischio sismico e recentemente ha subito i forti terremoti del 2016 e del 2017: è quindi possibile che la torre sia stata danneggiata a causa del sisma.

L'obiettivo principale è la determinazione delle proprietà modali di questa costruzione storica in muratura utilizzando studi sperimentali e numerici. L'indagine sulla vibrazione ambientale ha permesso di eseguire un'analisi sperimentale, i cui risultati sono stati utilizzati per mettere a punto un modello numerico della struttura basato sull'analisi agli elementi finiti con elementi solidi. La calibrazione è stata effettuata in diverse fasi, modificando alcuni parametri come il modulo di elasticità, al fine di ottenere un modello numerico accurato che simuli il comportamento dinamico dell'intera struttura. Ottenendo una buona coerenza tra le analisi sperimentali e numeriche, lo studio ha rivelato le effettive proprietà dinamiche della torre.

Dall'analisi dei risultati ottenuti, è possibile fare considerazioni e trarre conclusioni circa i possibili danni nella struttura.

La raccolta di dati sul monitoraggio di strutture antiche e storiche può essere estremamente utile per identificare danni e pianificare interventi e contribuire alla protezione e al mantenimento del patrimonio culturale.

Table of Contents

Ringraziamenti

Abstract

Riassunto

1. Introduction	1
1.1 Motivation	1
1.2 State of the art	2
1.3 Focus and objectives of the thesis	3
1.4 Outline of the thesis.....	3
2 The case study: Ostra Civic Tower	5
2.1 Description of the tower and historical background	5
2.2 Geometrical and material survey.....	9
2.3 Masonry quality index (MQI)	15
3 Operational modal analysis.....	25
3.1 Modal analysis	25
3.1.1 Mathematical formulation.....	26
3.2 Ambient modal identification.....	30
3.2.1 Methods.....	31
3.2.1.1 Frequency domain decomposition (FDD) and enhanced frequency domain decomposition (EFDD)	32
3.2.1.2 Stochastic Subspace Identification (SSI) method.....	32
3.2.2 Measurement procedures.....	33
3.2.2.1 Equipment	34
3.2.2.2 Measurement setups	36
3.2.2.3 Experimental results.....	38

3.2.3	Modal parameters estimation using Artemis modal pro software	46
3.3	A comparison between two softwares for OMA: ARTeMIS and ModalVIEW	56
4	Finite element modelling of the tower	65
4.1	Initial numerical model of the tower	65
4.2	Modal updating procedure	71
4.2.1	First step of calibration.....	71
4.2.2	Second step of calibration	74
4.2.3	Third step of calibration	77
4.2.4	Sensitivity analysis.....	80
4.2.5	Last step of calibration	81
4.2.5.1	Modal Assurance Criterion (MAC).....	84
4.3	Calibration using Midas FEA.....	86
4.4	Identification of structural damage.....	88
5	Conclusions and prospects	91
	References.....	95
	Publication.....	101

Chapter 1

Introduction

1.1 Motivation

The recent seismic events that affected many regions in Italy showed how vulnerable this territory and its buildings are. The damage to structures due to earthquakes is often significantly relevant; in particular, ancient constructions are the most involved and damaged. Considering that Italy is characterised by a huge number of cultural heritage buildings, it is crucial to guarantee their appropriate maintenance and to take preventive actions in order to avoid irreparable damage or collapse. An enhanced knowledge of dynamic behaviour of structures is a critical issue for the success in damage detection and it can play a relevant role in defining proper countermeasures for existing buildings and historical structures. Monitoring tools can be of great help in terms of static and dynamic characterization as reliable non-destructive methods and are useful especially when there the preservation of the historical value of the construction must be guarantee.

For all these reasons, many studies and much effort have been devoted to the improvement of dynamic identification techniques and health monitoring of buildings in the last few years. Nevertheless, a great deal of work is required to make these tools completely reliable and to broaden their applicability.

The present work is based on these remarks and attempts to contribute to the field of structural damage detection of buildings by studying the dynamic behaviour based on experimental data and numerical models of a case study.

1.2 State of the art

The maintenance and preservation of architectural heritage requires a compromise between the structural safety and the attention to the architectural and cultural value. The historical and architectural heritage, mainly made of masonry structures, is characterized by a wide range of uncertainties, such as masonry irregularities and imperfections, local variability of material strength and stiffness as well as the effects of past damages and repairs [1]. In addition, buildings can be damaged by environmental stressors and unexpected excitations caused natural disasters, such as earthquakes or typhoons.

Damage is defined as the deviation in original material or geometric properties causing displacements, vibrations or undesirable stresses. To ensure the safety of buildings, by continuous maintenance and repair works for the structures when required, damage detection is one of the primary task to be applied for this purpose. Therefore, several techniques for the observation of the dynamic behaviour of structures, known as structural health monitoring (SHM), have been developed [2-4].

In particular, the damage detection is one of the primary task in order to ensure the safety of buildings. In this context, the evaluation of the structural response at low/moderate vibration amplitude is of interest as structural damage diagnosis method.

The basic idea of a vibration-based damage detection method is that changes in physical properties of materials will cause damages in the measured dynamic response of the structure on modal parameters [5-11].

To this end, a grid of sensors, deployed along a structure, each one communicating with a central processing unit through wired or wireless connection, can be used [12-14]. Data collected by sensors are stored in central unit memory and then post-processed to determine the modal parameters of the structure in operational conditions. To this aim, operational modal analysis (OMA) is an efficient method to be used to this purpose, as it is able to estimate the modal parameters of the structure in a non-invasive way [15-16,37].

1.3 Focus and objectives of the thesis

This thesis envisages applying a SHM technique for the dynamic identification of the Civic Tower of Ostra. The technique is based on the ambient modal identification, also known as Operational Modal Analysis (OMA), and aims at identifying the modal properties of a structure based on vibration data collected when the structure is under its operating conditions, so that no initial excitation or artificial excitation is set.

As a first objective, in order to obtain the response needed for the OMA, a measurement procedure, in which several sensors are placed on the structure and then moved from position to position, has been defined so that multiple measurements could be performed. The second objective of the thesis was to build a 3D Finite Element model of the tower and to derive a model updating procedure that consists of iteratively changing updated parameters to make the structure better match the target responses. In this way, an updated FE mock-up can represent current realistic behaviour of the structure.

1.4 Outline of the thesis

The present thesis is structured as follows: Chapter 2 describes the Civic Tower of Ostra from a historical and geometrical point of view. After a brief introduction on the history of the tower, its origin and its reconstruction, the geometrical survey is explained in details and all the materials that compose the tower are listed. Plans, elevations and sections help to understand the all structure.

Chapter 3 illustrates the operational modal analysis (OMA), also called ambient modal identification or output-only modal analysis. The mathematical formulation of this analysis is reported together with some principal methods for ambient modal identification. The importance of this chapter lies in the explanation of the monitoring campaign and its results. Two different software were used to perform the modal analysis: ARTeMIS Modal Pro e ModalVIEW.

Chapter 4 presents the finite element method and the modal updating procedure used to calibrate the numerical model of the tower. The all process is explained in details, from the building of the initial model to the final step of calibration. Figures and tables report

the results of each step. In the end, a brief discussion on the identification of structural damage is reported.

Finally, Chapter 5 summarizes the conclusions that are drawn from this study and presents the key conclusions of each chapter. It also illustrates the practical aspects and challenges related to the implementation of a modal-based structural health monitoring.

Chapter 2

The case study: Ostra Civic Tower

2.1 Description of the tower and historical background

The bell-tower is located in the city of Ostra, a small Italian town 40 km far from Ancona. It is known as the Civic-tower of Ostra and it is considered the major symbol of the city: from the top one can admire a beautiful Marche landscape.

Lying on one of the characteristic hills of the Marche countryside, overlooking the Misa valley, Ostra was called Montalboddo until 1881 and, according to tradition, it was founded by the exiles of the Roman city of Ostra destroyed by the invasions of the Goths. The medieval city wall, 1200 meters long, surrounds the city, interspersed with square towers, nine of which still exist today.

The tower stands in the central Piazza dei Martiri, the upper part of the historic centre, at the confluence of Via del Teatro, Corso Mazzini and Via Gramsci. Piazza dei Martiri is the heart of city life and the main square of the Municipality. The eighteenth century Palazzo Comunale overlooks it, with the adjoining La Vittoria Theatre and the Church of San Francesco.

Built in the XVI century, the Civic Tower of Ostra is also known as the “Clock Tower”: inside the ancient gears of the clock are still preserved but they are no longer in operation. The bell also is still present and dates back to 1631.



(a)



(b)

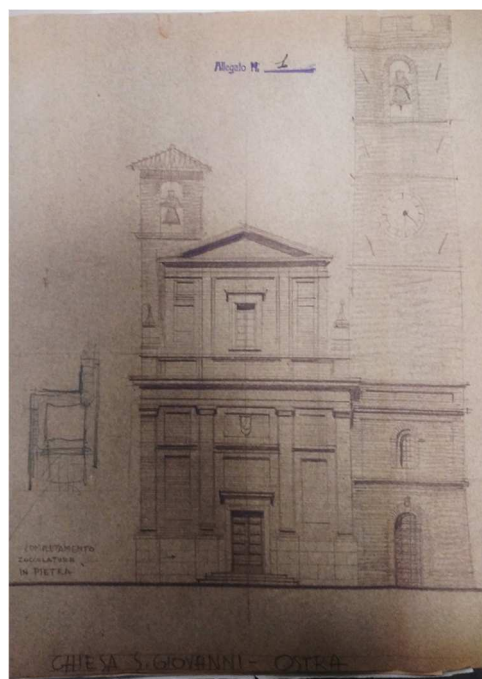
Figura 2.1 – (a) A view of Piazza dei Martiri and of the Civic Tower that overlooks it. (b) A photo of the original mechanism of the clock.

The belfry was originally annexed to the no longer existing church of San Giovanni: in the late spring of 1944 with the raging of the war and as a result of an aerial bombardment the old church of San Giovanni was hit and almost completely destroyed. Only the facade of the church and the civic tower survived the bombardment and with the alternation of seasons, they have become increasingly precarious. Hence the need, recognized by the senior technical offices, to demolish the facade and reinforce the tower and to consequently rearrange the area of the former church of San Giovanni.

The two buildings had autonomous origins: the church is remembered for the first time in archival documents in 1454, while the Tower was built in 1552 at the behest of the magistracy. With its double staircase, the church closed the fourth side of the square, helping to make it an elegant living room. Inside, among the various art objects, the church held various altarpieces including that of Andrea Sacchi (1599/1661) depicting San Bonaventura da Bagnoregio and San Tommaso d'Aquino (now at the Superintendency of Urbino) and "La Beata Vergine del Carmine" by Carlo Maratta (1625/1713) now in San Francesco church.



(a)



(b)

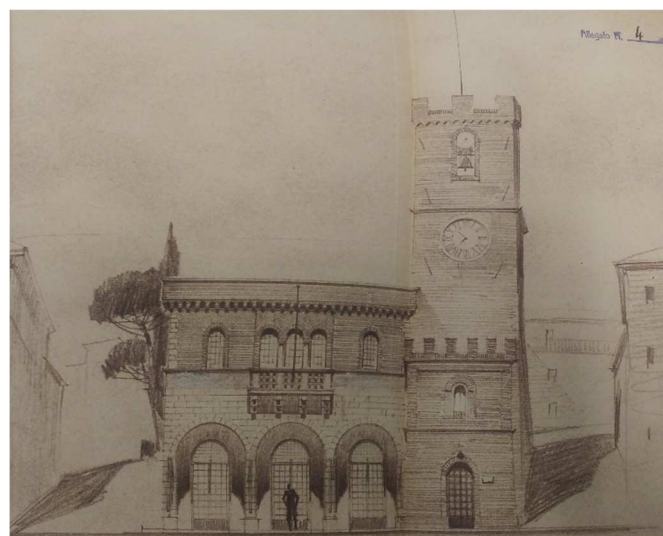
Figura 2.2 – (a) A photo of San Giovanni church and the Civic Tower before the bombardment. (b) A drawing of San Giovanni church and the Civic Tower found in the State Archives of Ancona.

As a consequence of the demolition of the façade of San Giovanni church, the foundations of the tower walls and the external staircase, adjacent to the perimeter walls of the building, remained uncovered above a clay bench. Since in this way the foundations were exposed to atmospheric agents, the stability of the important tower construction could have been quickly compromised. It was therefore necessary to carry out foundation works and recovery of the base walls promptly. Some parts of the external walls and of the battlement, damaged by the bursts of artillery bullets, were also restored.

The architectural arrangement of the square had also become indispensable. Some projects envisaged creating a decent background, in harmony with the palaces that frame the town square, and erecting a building that would replace the beautiful demolished façade and which, with the civic tower, formed a single architectural complex, majestic and harmonious.



(a)



(b)

Figura 2.3 – (a) A project of 1950 that planned the reconstruction of the tower and included the construction of a secondary school and a post office. (b) Another project of 1950 that proposed the construction of a building for public functions.

The city council finally approved the project to build an exedra in the aforementioned area with access steps and supporting wall of the overlying road with a background of evergreen tall trees. This solution, also approved by the Superintendence of Monuments, did not affect the municipal budget, as the relative expenses were assumed by the State

for war damage inherent in the strengthening of the tower and the arrangement of the adjacent Piazza dei Martiri.

To date, the tower cannot be visited because the staircase to climb the upper floors is precarious and unsafe. An invitation to tender has recently been published with the aim to make it accessible.

2.2 Geometrical and material survey

The Civic Tower of Ostra is circa 30 meters high: originally, it measured 25 meters, but after the interventions in 1950, the foundations were built and the tower was raised even more upwards.

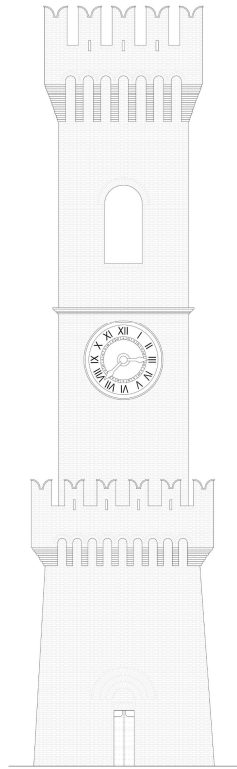
From the exterior, the structure can be divided into four parts: the basement, the central body, the belfry and the top. The basement and the top did not exist originally, so they are new parts, built in the 50s. The belfry, where the bell lies, is original while the central body has been partially reconstructed.

The basement consists of a truncated pyramid whose lower base measures approximately $7.30 \times 7.50 \text{ m}^2$ while the upper base is $5.30 \times 5.60 \text{ m}^2$. The central part of the tower is parallelepiped and widens at the top with characteristic battlements.

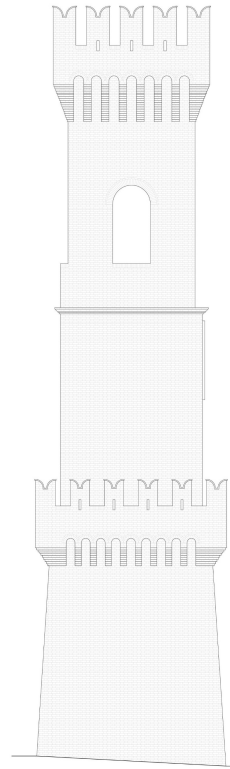
The tower rises on 5 floors: the first 3 floors are reached by spiral staircases, while to reach the 4th and 5th floors it is necessary to climb on iron ladder.

The entrance is on the north-east side which overlooks Martiri's square and it is the main façade.

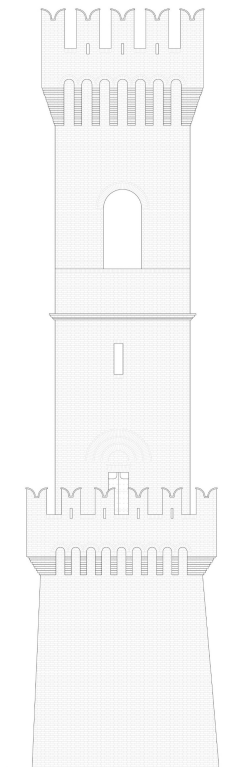
Only a wooden spiral staircase that leads to the first floor characterizes the ground floor. On the first floor, a terrace surrounds the entire perimeter of the tower at the height of nine meters and a half and battlements identify it. Going upstairs one can reach the old clock mechanism that is no longer in use today. The third floor is the belfry, characterized by four arched openings and the presence of the bell. Before reaching the top floor, a beautiful terrace 28 meters high, there is an intermediate level where one can rest after climbing the iron ladder.



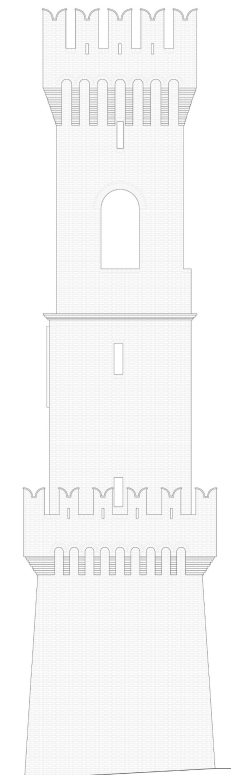
North elevation



East elevation



South elevation



West elevation

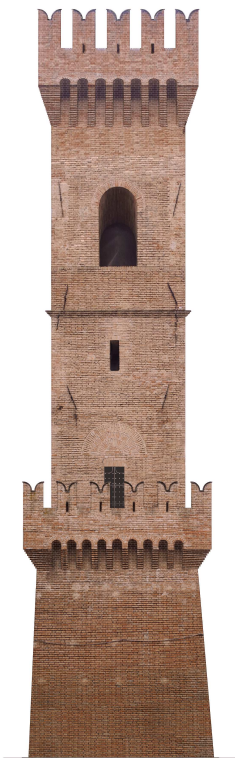
0 1 2 3 4 5 meters



North elevation



East elevation

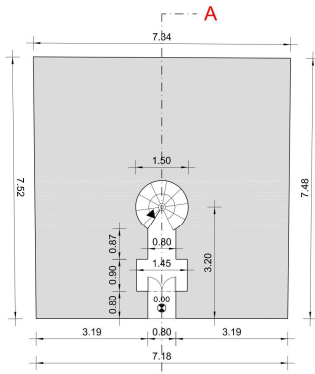


South elevation

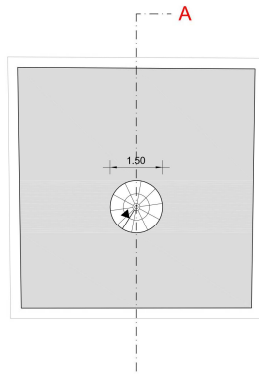


West elevation

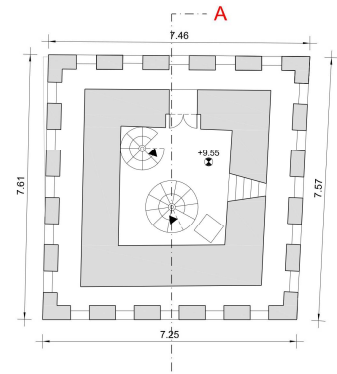
0 1 2 3 4 5 meters



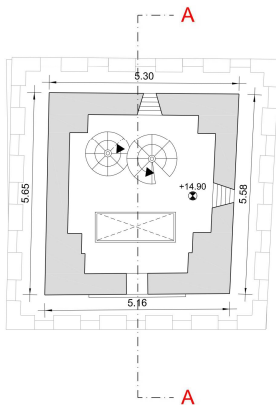
Ground floor



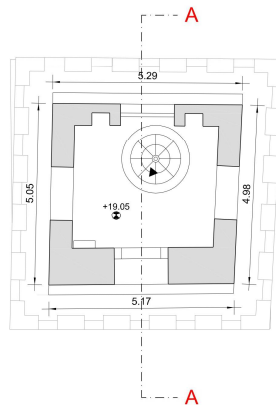
Intermediate level



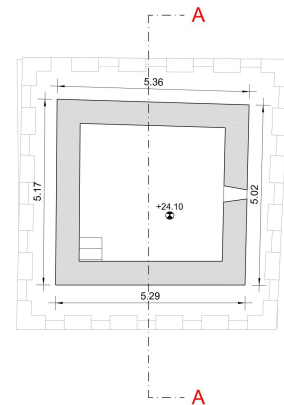
1st floor



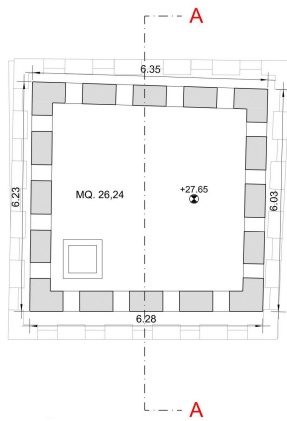
2nd floor



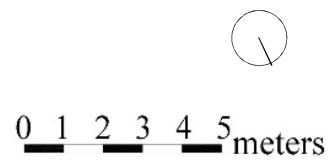
3rd floor

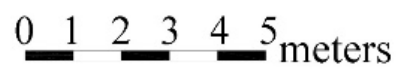
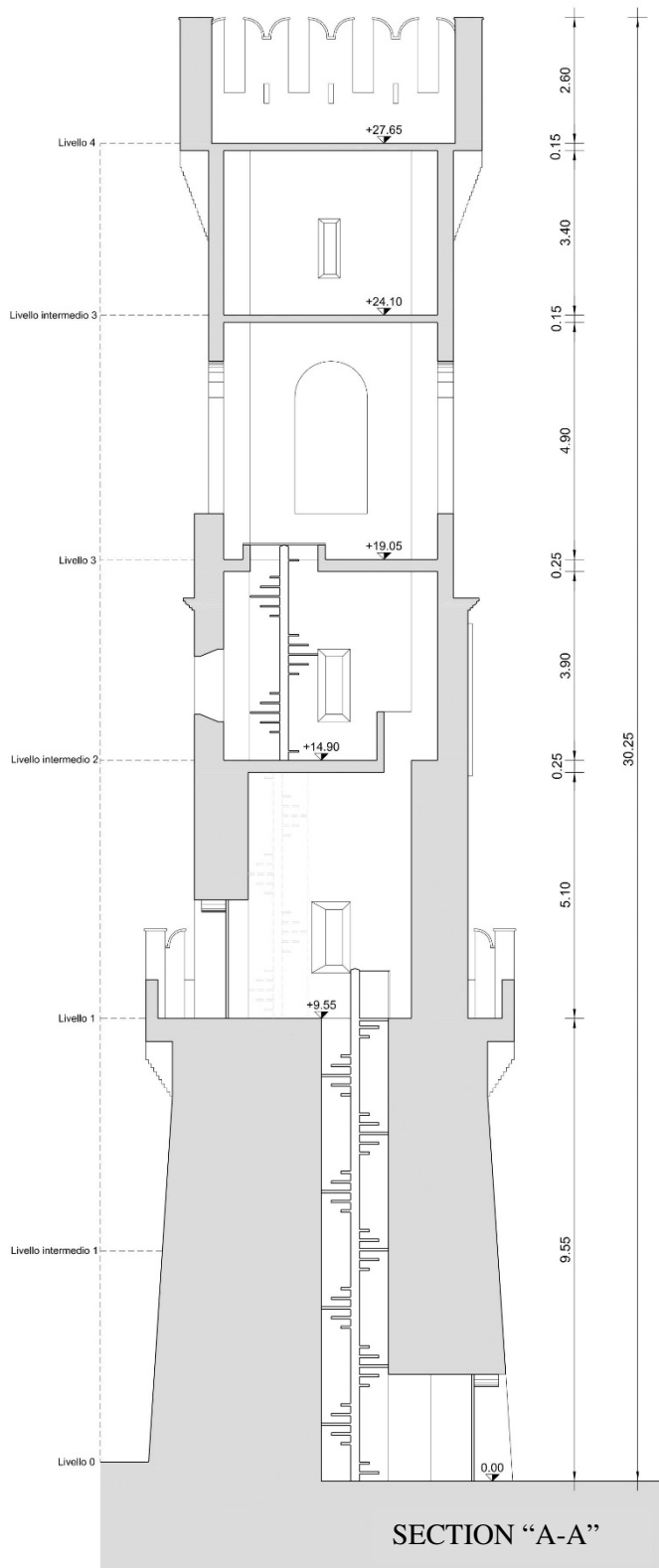


4th floor



5th floor





Different materials can be distinguished in the tower. In detail, the walls are made out of solid brick masonry with thin mortar joints and inner rubble core, whereas the slabs are built in reinforced concrete, revealing the recent replacement of this part. On the second and third floors, there are reinforced concrete columns on the corners.

The thickness of the walls ranges from 1.1 m of the lower part to 0.6 m of the upper part, while the thickness of the slabs varying from about 0.11 m to 0.27 m.

Another important thing to notice is the presence of iron tie-rods identified by anchor plates on the four facades. They were installed after the seismic events that affected the Marche region in order to avoid out-of-plane bending. However, the tower has no evident or worrying cracks or lesions.

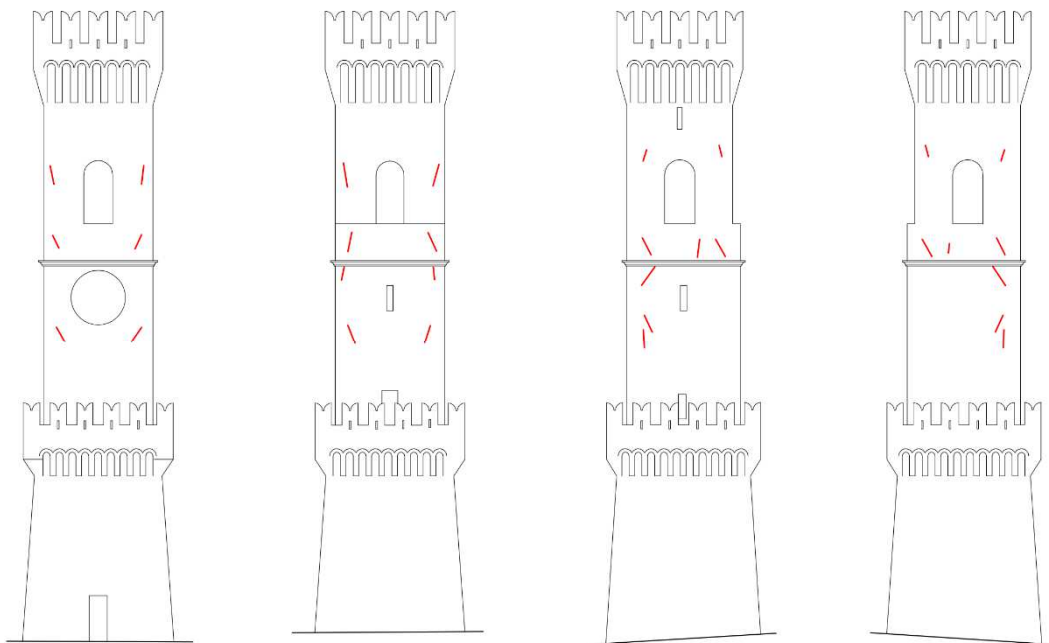


Figura 2.4 – The figure shows the anchor plates of the tie-rods in red colour

2.3 Masonry quality index (MQI)

The Masonry Quality Index is a method for the evaluation and classification of historic masonry [25]. It defines if the masonry is executed following the so-called “rules of the art”, which ensure good behaviour, monolithicity and compactness. This method is based on a qualitative evaluation of the masonry of a building and can be carried out without any need of instruments but just carefully observing the execution of the walling. It is therefore helpful if in situ tests or semi-destructive methods are not allowed, especially for the buildings belonging to the historical and cultural Heritage. The mechanical behaviour of masonry material depends on many parameters, such as block shape, compressive and shear strength of mortar and blocks, and the difficulty involved in the determination of these characteristic is often high. The method here presented envisages supporting the analysis of the masonry quality.

The index MQI is defined as

$$MQI = SM(SD + SS + WC + HJ + VJ + MM)$$

where SM, SD, SS, WC, HJ, VJ, MM are seven parameters considered for the evaluation of the mechanical properties of a masonry wall and are explained in the following Tables. All criteria are based on qualitative analysis.

NF	Degraded/damaged elements (>50% of total number of elements) Hollow bricks (solid < 30%) Mud bricks Unfired bricks
PF	Presence of degraded/damaged elements (≥10%, ≤50%) Hollow bricks (55 ≥ solid ≥ 30%) Sandstone or tuff elements
F	Un-damaged elements of degraded/damaged elements <10% Solid fired bricks Hollow bricks (55% < solid) Concrete blocks Hardstone

Table 2-1 – SM parameter: criteria for analysis of stone/brick mechanical properties

NF	Presence of more than 50% of elements with large dimension < 20cm Brick bond pattern made of only head joints
PF	Presence of more than 50% of elements with large dimension 20–40cm Co-presence of elements of different dimensions
F	Presence of more than 50% of elements with large dimension > 40cm

Table 2-2- SD parameter: criteria for analysis of stone/brick dimensions

NF	Rubble, rounded or pebble stonework (predominant) on both masonry leaves
PF	Co-presence of rubble, rounded or pebble stonework and barely/perfectly cut stone and bricks on both masonry leaves One masonry leaf made of perfectly cut stones or bricks Masonry made of irregular (rubble, rounded, pebble) stones, but with presence of pinning stones
F	Barely cut stones or perfectly cut stones on both masonry leaves (predominant) Brickwork

Table 2-3 – SS parameter: criteria for analysis of stone/brick shape

	Visible section (quantitative analysis)	Non-visible section (qualitative analysis)
NF	MI < 1.25 Small stones (for any MI value)	Small stones compare to wall thickness No headers
PF	1.25 < MI < 1.55	For double-leaf wall Presence of some headers Wall thickness larger than stone large dimension
F	MI > 1.55	Wall thickness similar to stone large dimension Systematic presence of headers

Table 2-4 – WC parameter: criteria for analysis of wall leaf connections. MI

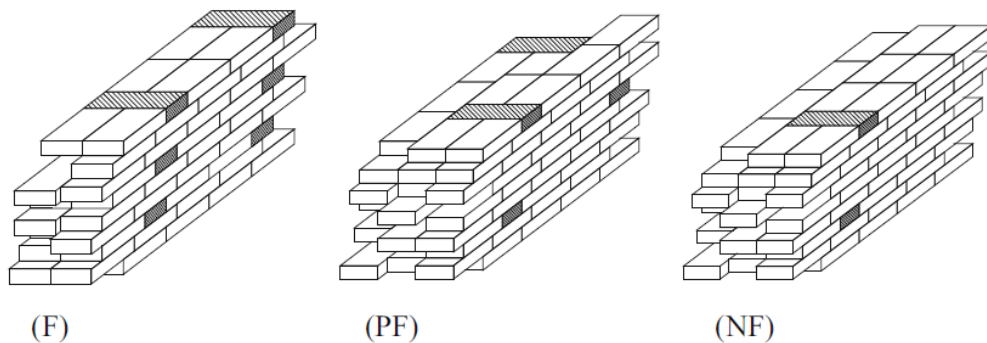


Figura 2.5 – Wall leaf connections (WC)

NF	Bed joints not continuous
PF	Intermediate situation between NF and F For double-leaf wall Only one leaf with continuous bed joints
F	Bed joints continuous Stone masonry wall with bricks courses (distance between courses < 60 cm)

Table 2-5 – HJ parameter: criteria for analysis of horizontality of bed joints

Quantitative analysis		
NF	Single-leaf wall ($MI < 1.4$)	Aligned vertical joints
	Double-leaf wall ($MI < 1.4$ for one masonry leaf, $MI < 1.6$ for the second one)	Aligned vertical joints for at least 2 large stones Solid brick wall made of only headers
	Wall made of very small stones	
PF	Single leaf wall $1.4 < MI < 1.6$	Partially staggered vertical joints
	Double-leaf wall	(vertical joint between 2 brick is not placed in the middle of adjacent upper and lower brick)
	(a) Both leaves $1.4 < MI < 1.6$	
	(b) For at least one leaf $MI > 1.6$	
	(c) First leaf $MI > 1.6$	
	(d) Second leaf $1.4 < MI < 1.6$	
F	Single leaf wall $MI > 1.6$	Properly staggered vertical joints
	Double-leaf wall (both leaves $MI > 1.6$)	(vertical joint between 2 stones is placed in the middle of adjacent upper and lower stone)

Table 2-6 – VJ parameter: criteria for analysis of stagger properties of vertical joints

NF	Very weak mortar, dusty mortar with no cohesion No mortar (rubble or pebble stonework) Large bed joints made of weak mortar (thickness comparable to stone/brick thickness) Porous stones/bricks with weak bonding to mortar
PF	Medium quality mortar, with bed joints not largely notched Masonry made of irregular (rubble) stones and weak mortar, but with presence of pinning stones
F	Good quality and non-degraded mortar, regular bed joint thickness or large bed joint thickness made of very good quality mortar Masonry made of large perfectly cut stones with no mortar or very thin bed joint thickness

Table 2-7 – MM parameter: criteria for analysis of mortar properties

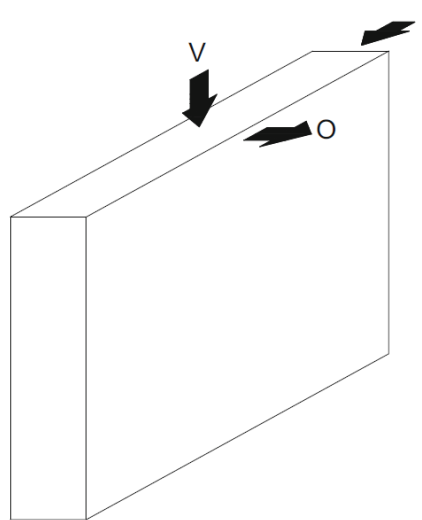


Figura 2.6 – Load conditions. V vertical loads; O out-of-plane loads, I in-plane loads

The numerical value given to each parameter is illustrated in Table 2-8

	Vertical loading (V)			Horizontal in-plane loading (I)			Horizontal out-of-plane loading (O)		
	NF	PF	F	NF	PF	F	NF	PF	F
HJ	0	1	2	0	0.5	1	0	1	2
WC	0	1	1	0	1	2	0	1.5	3
SS	0	1.5	3	0	1	2	0	1	2
VJ	0	0.5	1	0	1	2	0	0.5	1
SD	0	0.5	1	0	0.5	1	0	0.5	1
MM	0	0.5	2	0	1	2	0	0.5	1
SM	0.3	0.7	1	0.3	0.7	1	0.5	0.7	1



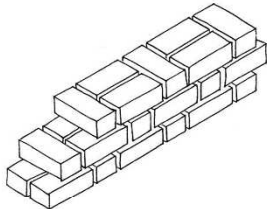
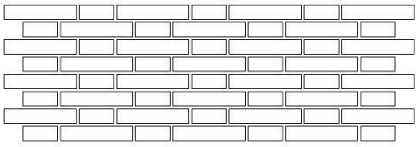
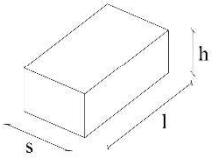
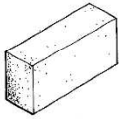
Table 2-8 – numerical values for analysis


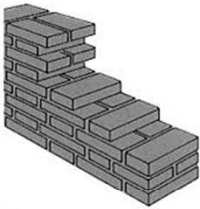
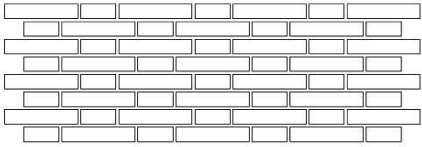
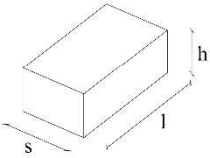
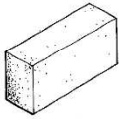
Based on the MQI values, the masonry is classified in three categories (Table 2-9)



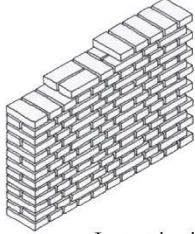
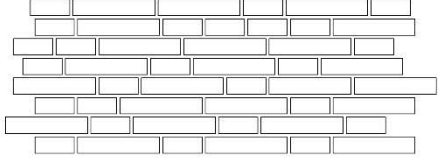
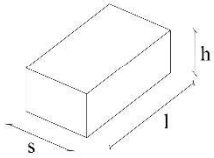
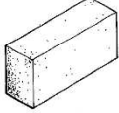
Masonry category	Masonry category		
	C	B	A
Vertical actions (V)	$0 \leq \text{MQI} \leq 2.5$	$2.5 \leq \text{MQI} \leq 5$	$5 \leq \text{MQI} \leq 10$
Out-of plane actions (O)	$0 \leq \text{MQI} \leq 4$	$4 \leq \text{MQI} \leq 7$	$7 \leq \text{MQI} \leq 10$
In-plane actions (I)	$0 \leq \text{MQI} \leq 3$	$3 \leq \text{MQI} \leq 5$	$5 \leq \text{MQI} \leq 10$



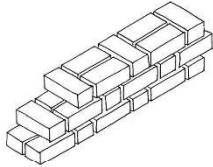
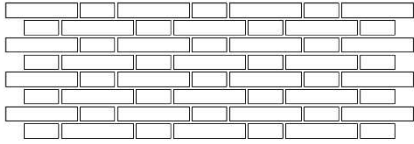
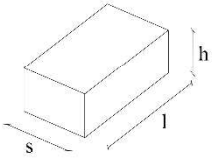
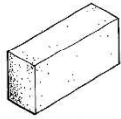
Table 2-9- masonry categorie sas a function of the MQI. A, good behaviour of masonry. B, behaviour of average quality of the masonry; C, inadequate behaviour of masonry

The cards reported in the following pages illustrate the application of the method to the types of masonry walls present in the tower.

		 					PHOTOS			
		 					LAYOUT			
		<p><i>Double-leaf brick wall</i></p> <p>Masonry leaves are made of parallelepiped bricks. Systematic presence of headers. Horizontally of bed joints fulfilled. Partially staggered vertical joints.</p> <p>Good-quality firebricks. Regular bed joints thickness made of good quality mortar (cement mortar).</p>					DESCRIPTION MATERIALS			
		 <p>Dimensions and typical shapes of blocks:</p> <p>$s = 12 \div 13$ cm $h = 5 \div 6$ cm $l = 25 \div 27$ cm</p> 					GEOMETRY			
SM	SD	SS	WC	HJ	VJ	MM	Vertical	Horizontal in-plane	Horizontal out-of-plane	ANALYSIS
F	PF	F	F	F	PF	F Category	A	A	A	
MQI							9	8,5	9	
Mech. properties (min-max)							f_m (MPa)	E (MPa)	τ_0 (MPa)	
							7,02-11,70	3510-5260	0,15-0,22	

							PHOTOS					
												
 <p style="text-align: center;">Isometric view</p>							 <p style="text-align: center;">Front view</p>			LAYOUT		
<p><i>Brick wall made out of three headers</i></p> <p>Masonry leafs are made of parallelepiped bricks. Typical flemish bond masonry. Horizontally of bed joints fulfilled. Partially staggered vertical joints.</p> <p>Medium-quality firebricks. Regular bed joints thickness.</p>							DESCRIPTION			MATERIALS		
 <p style="text-align: center;">Dimensions and typical shapes of blocks:</p> <p>$s = 12 \div 13 \text{ cm}$ $h = 5 \div 6 \text{ cm}$ $l = 25 \div 27 \text{ cm}$</p> 							GEOMETRY					
SM	SD	SS	WC	HJ	VJ	MM	Vertical	Horizontal in-plane	Horizontal out-of-plane	ANALYSIS		
F	PF	F	PF	F	PF	F Category	A	A	A			
MQI							9	7,5	7,5			
Mech. properties (min-max)							f_m (MPa)	E (MPa)	τ_0 (MPa)			
							7,02-11,70	3510-5260	0,15-0,22			

		 					PHOTOS			
		 					LAYOUT			
		<p><i>Double-leaf brick wall</i></p> <p>Masonry leaves are made of parallelepiped bricks. Systematic presence of headers. Bed joints continuous. Partially staggered vertical joints.</p> <p>Presence of damaged elements Medium quality mortar, with bed joints not largely notched.</p>					DESCRIPTION MATERIALS			
		<p>Dimensions and typical shapes of blocks:</p>  <p>$s = 12 \div 13$ cm $h = 5 \div 6$ cm $l = 25 \div 27$ cm</p> 					GEOMETRY			
SM	SD	SS	WC	HJ	VJ	MM	Vertical	Horizontal in-plane	Horizontal out-of-plane	ANALYSIS
PF	PF	F	F	F	PF	PF	A	A	A	
MQI							5,25	5,25	5,95	
Mech. properties (min-max)							f_m (MPa)	E (MPa)	τ_0 (MPa)	
							4,68-7,80	2340-3510	0,15-0,22	

						PHOTOS						
						LAYOUT						
		Isometric view		Front view		DESCRIPTION MATERIALS						
		<p><i>Double-leaf brick wall</i> Masonry leafs are made of parallelepiped bricks. Systematic presence of headers. Horizontally of bed joints fulfilled. Partially staggered vertical joints.</p> <p>Good-quality firebricks. Regular bed joints thickness made of good quality mortar (cement mortar).</p>										
				Dimensions and typical shapes of blocks: $s = 12 \div 13 \text{ cm}$ $h = 5 \div 6 \text{ cm}$ $l = 25 \div 27 \text{ cm}$				GEOMETRY				
SM	SD	SS	WC	HJ	VJ	MM		Vertical	Horizontal in-plane	Horizontal out-of-plane	ANALYSIS	
F	PF	F	F	F	PF	F	Category	A	A	A		
							MQI	9	8,5	9		
							Mech. properties (min-max)	f_m (MPa)	E (MPa)	τ_0 (MPa)		
								7,02-11,70	3510-5260	0,15-0,22		

Chapter 3

Operational modal analysis

3.1 Modal analysis

Modal analysis is the study of the dynamic behaviour of a structure when it is subject to vibration. In structural analysis, it allows the determination of the properties and response of a structure, constrained or free, in autonomous dynamics or excited by dynamic forcing stresses imposed from the outside.

In the case of simple bodies, the modal analysis is able to study the dynamic behaviour in detail through the evaluation of its natural frequency and of the associated vibrating modes. In the case of complex structures, they are previously schematized through the finite element method. This analysis defines the response of the structure to forcing with different harmonic contents. The fields of application of this methodology are various: with regard to civil engineering, the purpose is to carry out a seismic analysis.

Modal analysis separates the complicated vibration pattern that can be measured in a physical domain into a set of modes of vibration. These modes are, we can say, the “fingerprint” of a structure.

The modal properties of a structure include primarily the natural frequencies, damping ratios and mode shapes. These three parameters characterize a mode of vibration. A

structure typically has many modes of vibration that normally get more and more complicated in shape as the frequency gets higher and it normally require more energy to excite these modes compared to the more simple low frequency modes.

3.1.1 Mathematical formulation

The dynamic problem, with N degrees of freedom, is described by N differential equations in N unknowns: these equations are coupled - all the unknowns appear in all the equations - so to solve the system it is necessary to decouple it and thus have only one unknown in each equation. The dynamic modal analysis is used precisely to decouple the system and solve the equations.

In the case of seismic force, in which the system is subjected to a motion at the foundation described by the time-history $u_g(t)$, the vector of the total displacements of the masses is given by

$$\mathbf{X}(t) = \mathbf{U}(t) + u_g(t)\mathbf{R} \quad (1)$$

where \mathbf{R} defines the displacement component for each degree of freedom due to the rigid displacement of the structure. The equation of motion of the system is therefore:

$$\mathbf{M}\ddot{\mathbf{U}}(t) + \mathbf{C}\dot{\mathbf{U}}(t) + \mathbf{K}\mathbf{U}(t) = -\mathbf{M}\mathbf{R}\ddot{u}_g(t) \quad (2)$$

$$\mathbf{M} = \begin{bmatrix} m_1 & & \\ & \dots & \\ & & m_n \end{bmatrix} \quad \mathbf{K} = \begin{bmatrix} k_{11} & \dots & k_{1n} \\ \dots & \dots & \dots \\ k_{n1} & \dots & k_{nn} \end{bmatrix} \quad \mathbf{C} = a_0\mathbf{M} + a_1\mathbf{K}$$

Mass matrix
(diagonal matrix)
Stiffness matrix
(full symmetric and
positive-definited matrix)
Dissipation matrix
(damped systems)

The dynamics of linear systems with multiple degrees of freedom can be studied by identifying the modes of vibrating that derive from the study of free oscillations of the system. The free oscillations of the system derive from having imposed, at the time $t = 0$, non-zero displacements and / or non-zero velocities to the masses. The applied forces are null. The resolving system can be written in matrix form

$$\begin{array}{ll} \text{Equation of} & \mathbf{M}\ddot{\mathbf{U}}(t) + \mathbf{K}\mathbf{U}(t) = 0 \\ \text{motion} & \end{array} \quad \begin{array}{l} \text{Initial} \\ \text{conditions} \end{array} \quad \begin{cases} \dot{\mathbf{U}}(0) = \dot{\mathbf{U}}_0 \\ \mathbf{U}(0) = \mathbf{U}_0 \end{cases}$$

The solutions searched are those in which the oscillations occur according to a harmonic motion separating the time variable from the "form" of the vector of the displacements

$$\mathbf{U}(t) = \Phi \cos(\omega t - \varphi) \quad (3)$$

where Φ is the vector of the displacements of the masses. Deriving twice the previous relation with respect to time, the acceleration vector is calculated as follows

$$\ddot{\mathbf{U}}(t) = -\omega^2 \Phi \cos(\omega t - \varphi) \quad (4)$$

Replacing the (4) in the equation of motion, the term $\cos(\omega t - \varphi)$ can be simplified

$$(\mathbf{K} - \omega^2 \mathbf{M})\Phi = 0 \quad (5)$$

The previous system of equations has non-zero solutions only if the following condition is verified

$$\det(\mathbf{K} - \omega^2 \mathbf{M}) = 0 \quad (6)$$

which is a m th (n th) degree polynomial equation with ω^2 as variable. Since \mathbf{K} and \mathbf{M} are symmetrical and positive-defined matrices, the m roots of the polynomial equation are real and positive and define the pulsations of m modes of vibration of the system.

To each pulsation ω_i corresponds a period $T_i = \frac{2\pi}{\omega_i}$

To each pulsation ω_i also corresponds a vector Φ_i (*eigenvector*) such that

$$(\mathbf{K} - \omega_i^2 \mathbf{M})\Phi_i = 0 \quad (7)$$

The equations of the system are not linearly independent and the solutions can be determined less than a constant. This is why eigenvectors define the so-called modal forms.

The eigenvectors are normalized to eliminate the uncertainty deriving from the definition of the constant. Various techniques can be used. The normalization is obtained by imposing the condition

$$\Phi_i^T \mathbf{M} \Phi_i = 1 \quad \rightarrow \quad \sum_{j=1}^n m_j \phi_{i,j}^2 = 1 \quad (8)$$

It can be demonstrated that the eigenvectors have the property of orthogonality with respect to mass matrix and the stiffness matrix, that is

$$\Phi_i^T \mathbf{M} \Phi_k = 0 \quad \Phi_i^T \mathbf{K} \Phi_k = 0 \quad (9)$$

A modal matrix is defined as the matrix whose columns are made up of modal forms

$$\mathbf{\Phi} = \begin{bmatrix} \phi_{1,1} & & \phi_{n,1} \\ \dots & \dots & \dots \\ \phi_{1,n} & & \phi_{n,n} \end{bmatrix} \quad \phi_{i,j} \text{ modal coefficient of the } i\text{-th mode on the } j\text{-th plane}$$

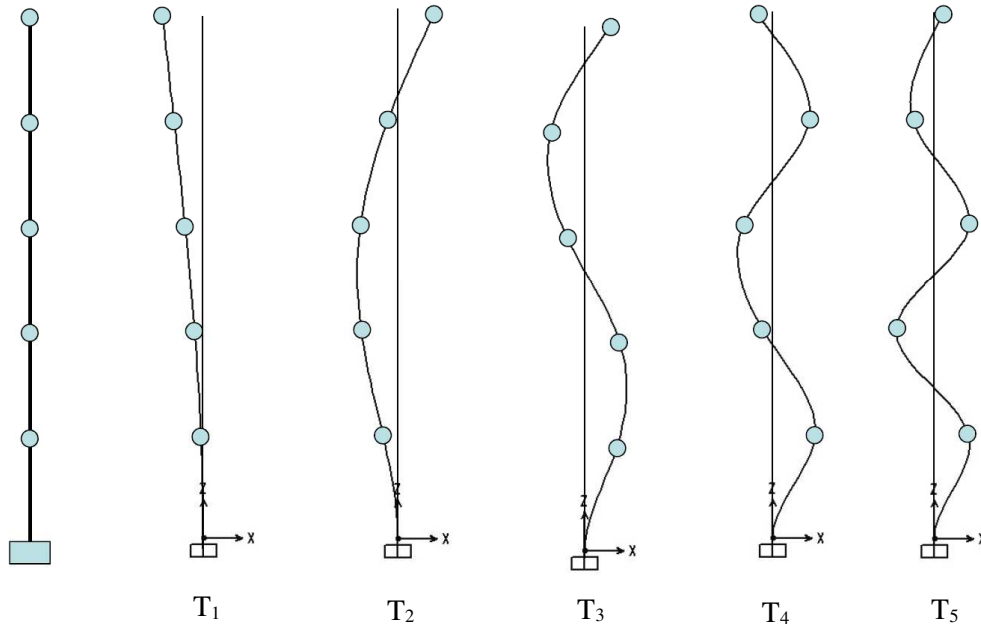
The following matrices are defined

$$\mathbf{M}^* = \mathbf{\Phi}^T \mathbf{M} \mathbf{\Phi} \quad \textit{generalized mass matrix}$$

$$\mathbf{K}^* = \mathbf{\Phi}^T \mathbf{K} \mathbf{\Phi} \quad \textit{generalized stiffness matrix}$$

Due to the property of the orthogonality of the eigenvectors of the mass matrix and the stiffness matrix, these matrices are both diagonal matrices

$$\mathbf{M}^* = \begin{bmatrix} M_1^* & & \\ & \dots & \\ & & M_n^* \end{bmatrix} \quad \mathbf{K}^* = \begin{bmatrix} K_1^* & & \\ & \dots & \\ & & K_n^* \end{bmatrix} \quad \text{where } M_i^* = \sum_{j=1}^n m_j \Phi_{i,j}^2 \quad \frac{K_i^*}{M_i^*} = \omega_i^2 M_i^*$$



The fundamental mode of vibrating of a structure is the one with the longest period.
 The generic vibration of the system is described by the linear combination of the n modes (which constitute the free periodic oscillations of the non-damped elastic system)

$$\mathbf{U}(t) = \sum_{j=1}^n z_j(t) \Phi_j = \Phi \mathbf{Z}(t) \quad z_j(t) - \text{generalized coordinates} \quad (10)$$

Replacing this relation in the equation of equilibrium, multiplying by Φ^T , and thanks to the property of orthogonality of the eigenvectors, it can be written

$$\mathbf{M}\ddot{\mathbf{U}}(t) + \mathbf{K}\mathbf{U}(t) = \mathbf{0} \quad (11)$$

$$\Phi^T \mathbf{M} \Phi \ddot{\mathbf{Z}}(t) + \Phi^T \mathbf{K} \Phi \mathbf{Z}(t) = \mathbf{0} \quad (12)$$

$$\mathbf{M}^* \ddot{\mathbf{Z}}(t) + \mathbf{K}^* \mathbf{Z}(t) = 0 \quad (13)$$

Since \mathbf{M}^* and \mathbf{K}^* matrices are diagonal, one can obtain a system of n decoupled equations, each of which represents the motion of the i-th mode

$$M_i^* \ddot{z}_i(t) + K_i^* z_i(t) = 0 \quad (14)$$

$$\ddot{z}_i(t) + \frac{K_i^*}{M_i^*} z_i(t) = 0 \quad (15)$$

$$\begin{cases} \ddot{z}_i(t) + \omega_i^2 z_i(t) = 0 \\ \dot{z}_i(0) = \dot{z}_{i0} \quad z_i(0) = z_{i0} \end{cases} \quad (16)$$

The n-degree-of-freedom (DOF) problem is transformed, in the system of the main coordinates, into n 1-dof problems relating to simple oscillators characterized by the pulsations ω_i .

3.2 Ambient modal identification

Ambient modal identification, also known as Operational Modal Analysis (OMA), aims at identifying the modal properties of a structure based on vibration data collected when the structure is under its operating conditions: no initial excitation or known artificial excitation is set.

It is also called output-only analysis because only vibration response is measured.

OMA techniques are conceived to work with free or ambient vibration recordings, where (small amplitude) vibrations may be well approximated by stationary Gaussian white noise. Although this does not reflect the reality, it is anyway a good approximation since the excitation can be seen as the response to a linear filter excited with white noise input. In an ambient vibration test the subject structure can be under a variety of excitation sources which are not measured but are assumed to be 'broadband random'.

One primary advantage of this technique is its implementation economy, as only the vibration of the structure needs to be measured. This is particularly attractive for civil engineering structures where it can be expensive or disruptive to carry out free vibration or forced vibration tests (with known input). Another benefit is the possibility of measuring the response of the structure using actual environmental excitations, such as wind or traffic.

The traditional experimental modal analysis (EMA), that is an input-output identification technique, contrary to OMA, estimates the modal parameters of structures based on the known artificial input force and recorded output responses. The input force is applied to the structures by shakers or impact hammers and the output responses are generally measured by accelerometers sensors. There are some shortcomings within EMA processes especially for civil engineering structures. Most civil engineering structures such as bridges, buildings, etc are under ambient loads like wind, traffic, pedestrian and since these loads are immeasurable, the input loads is not defined exactly. On the other hand, vibrating huge structures by shaker or impact hammer is very expensive and difficult, if not impossible. These reasons motivated researchers to identify the structures characteristics by considering just the response of the structure, regardless of input loads.

3.2.1 Methods

OMA methods can be categorized into time domain and frequency domain approaches. The techniques based on the analysis of response time histories are referred to as time domain methods. The frequency domain techniques are based on the relation between input and output power spectrum density (PSD). Frequency domain techniques for OMA purposes are not very popular due to the numerical conditioning issues. On the other hand, time domain methods are usually more suitable to handle noisy data, and they can avoid some signal processing errors, such as leakage.

3.2.1.1 Frequency domain decomposition (FDD) and enhanced frequency domain decomposition (EFDD)

This technique allows performing an approximate decomposition of the system response into a set of independent single degree of freedom (SDOF) systems, one for each mode. The decomposition is performed by simply decomposing each of the estimated spectral density matrices. The singular values are estimates of the auto spectral density of the SDOF systems in modal coordinates, and in the vicinity of the resonance peak the singular vectors are estimates of the mode shapes of the mode. The algorithm is based on three main steps: the estimation of the power spectral density matrix at discrete frequencies; the singular value decomposition of the power spectral density; for an n degree of freedom system, the picking of the n dominating peaks in the power spectral density using whichever technique you wish or manually. These peaks correspond to the mode shapes.

3.2.1.2 Stochastic Subspace Identification (SSI) method

The SSI method bases its technique using a difference equation based upon the raw time data.

This technique involves the use of statistics, optimal prediction, linear system theory and stochastic processes. It operates directly in time domain and is based on a state space description of the dynamic problem. The second-order problem stated by the differential equation of motion, is converted into two first-order problems, defined by the so-called “state equation” and “observation equation”.

The dynamic system is expressed in terms of inertial (mass), dissipative (damping) and restoring (stiffness) matrices. It is written in terms of a linear set of differential equations of the type:

$$[\mathbf{M}]\ddot{\mathbf{x}}(t) + [\mathbf{C}]\dot{\mathbf{x}}(t) + [\mathbf{K}]\mathbf{x}(t) = -\mathbf{f}(t) \quad (17)$$

By rewriting the equations of motion in a classical state-space formulation, the dynamic system is expressed as follows:

$$\begin{cases} x_{t+1} = [A]x_t + w_t \\ y_t = [C]x_t + v_t \end{cases} \quad (18)$$

where x_t represents the discrete time state vector yielding the sampled displacement and velocities. The first equation (state equation) represents the dynamic behaviour of the physical system and the second equation (observation equation) is called the output equation. The measured response y_t is generated by 2 stochastic processes w_t and v_t that represent the unmeasured and unknown noise processes. The matrix A is called the state matrix and the matrix C is called the observation matrix.

This technique uses a mathematical framework based on stochastic processes. A stochastic process is a mathematical modelling of a physical phenomenon that is not deterministic and is somehow not predictable from the knowledge of the present state of the system. The intrinsic randomness of the operational modal analysis technique makes stochastic techniques very suitable for modelling a physical system. The SSI technique works on the raw time data and tries to fit a model to the data captured from the responses at the degrees of freedom.

The idea behind the SSI technique is to be able to represent the system in Equation (18) in the frequency domain in terms of a Transfer Function that involves the matrices A , C , K , and the identity matrix. The eigenvalue decomposition of the matrix A leads to a representation of the transfer function matrix that contains the modal parameters (natural frequencies and damping ratios). The mode shapes are extracted from the eigenvectors of the matrix A and the observation matrix C .

3.2.2 Measurement procedures

There are two ways to measure in order to obtain the response needed for Operational Modal Analysis. Either all sensors are mounted once and the measurements are made, or the sensors are moved from position to position and multiple measurements are made. In the first case, the sensors are not moved and remain in the same position during all the measurement: they are placed ones in a *single test setup*. It is used in permanent monitoring or simply to save time. In the second case, the sensors are moved around from one set of positions to another set. There are always one or more sensor that remain fixed in the same position when moving from one setup to another: it provides a way to adjust

the rest of the mode shape values of the different test setups. This is a *multiple test setup* measurement procedure.

The procedure used in the present work is the second one. Four measurements were performed lasting 20 minutes each. One of the four sensor was not moved and remained fixed during all the four measurements; the other three sensors changed position from one measurement to another.

Moreover, structural health monitoring techniques can be subdivided into ‘continuous’ and ‘periodical’ monitoring. Continuous monitoring is a long term technique aimed to determine the natural structural degradation of the construction to ensure safety in service and to allow an economic and efficient maintenance programme. The periodical monitoring is a short term technique and can be used for periodical acquisition of data in order to define the structural response of the construction in a specific moment through the definition of dynamic parameters.

The present measurement campaign falls in the periodical monitoring, and the main objective is the extraction of structural dynamic parameters such as natural frequencies, damping ratios and mode shapes.

Two monitoring surveys were performed: one in June 29th,2018, and the other one in February 22nd,2019. The aim was to test the tower in two different weather conditions, with high temperatures and low temperatures.

3.2.2.1 Equipment

The sensor used for the monitoring survey were GEA II sensors marketed by Novatest Company.

The GEA System is based on digital triaxial accelerometers, distributed, with low background noise (<10 μg RMS in the band 0.1-50 Hz) and high dynamics (24 bit SigmaDelta AD converter). The digitalization on board of the sensor allows the installation of sensor networks (in the standard configuration up to 16 sensors) on areas with a radius of 1 km, guaranteeing data without disturbances of electromagnetic and / or triboelectric nature typical of analogue sensors. The great advantage of GEA sensors over conventional measurement solutions is that they can be directly connected to a computer with GEA Lab software installed, without the need for dedicated, proprietary memory cards.



Figure 3-1 – A photo of the sensors used for the monitoring survey

TECHNICAL FEATURES:

- *GEA2: Triaxial PIEZO-MEMS sensor*
- *Number of axles: 3*
- *Range: 8 g*
- *A / D converter: 24-bit SigmaDelta*
- *Sampling frequency: 1024 Hz*
- *Minimum measured level: 0.0005 mm / s*
- *Dynamic range: 120 dB*
- *Frequency range: 0.8-100 Hz (315 Hz)*
- *Protection degree: IP68*
- *Dimensions: D: 117 mm x H: 35 mm*
- *Material: Anodised aluminum*
- *Weight: 600 g*
- *Impact resistance: 3000 g*
- *Protection: IP68*
- *Operating temperature: -20 ÷ 75 ° C*

CHARACTERISTICS IN ACCELERATION:

SENSOR

- *Maximum measurable value: 8 g*
- *Spectral noise: 1 ug / hz-2 @ 1 hz*
- *Cross Axis Sensitivity: <5%*
- *Noise in the band (0-100 Hz): 15 µg*
- *Sensitivity: 1000 mV / g*

DYNAMIC

- *Frequency response: 0.8 - 600 Hz*
- *Resonance frequency: 16 kHz*
- *Sampling frequency: 1024 Hz*

- *Linearity: $\pm 1\%$ Max*
- *Dynamic range (of the sensor, in band): 120 dB*
- *AD Converter dynamic range (24 bit): 130 dB*

3.2.2.2 Measurement setups

As mentioned above, four 20-minute recordings were performed with a 1024 Hz sampling frequency and a 0.001 seconds sampling interval.

The accelerometers were placed in the corners of the tower and, from the top, two of them were moved a floor below at each recording, while the other two remained on the top. Only one of them stayed fixed during all the test setup. A scheme of the sensor positions is shown below.



Figure 3-2 – On the left, a photo of the central processor; on the right, two pictures of the positioning of the sensors

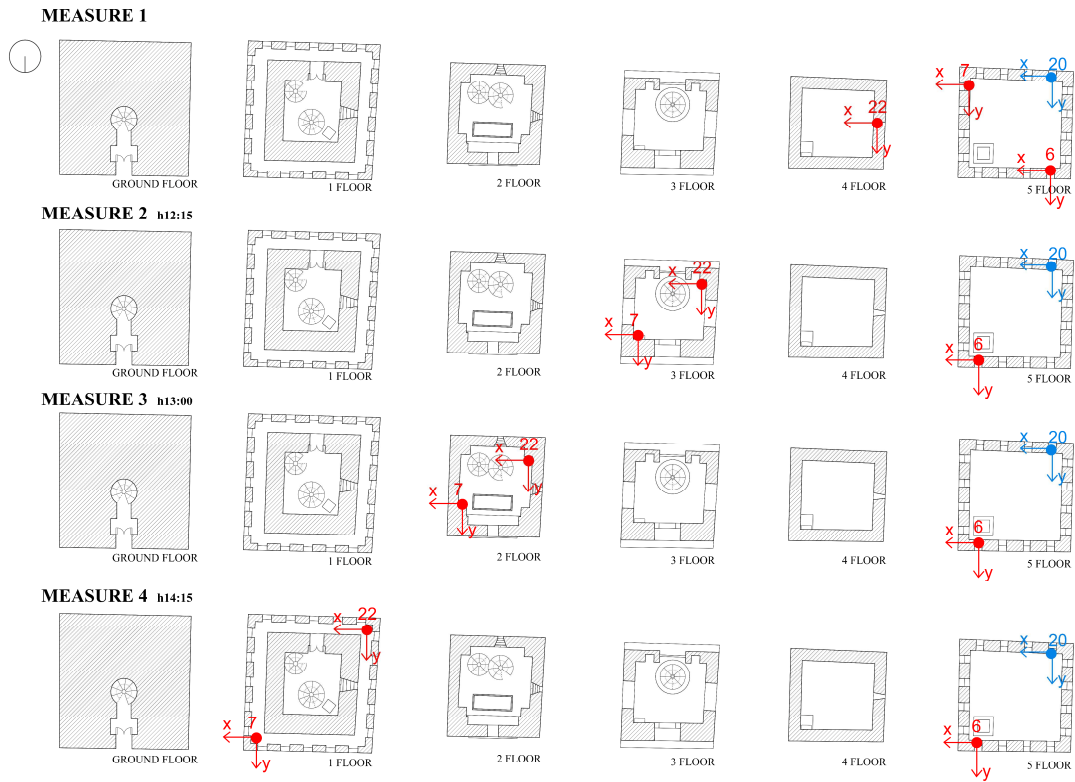


Figure 3-3 – Sensor positions in plan

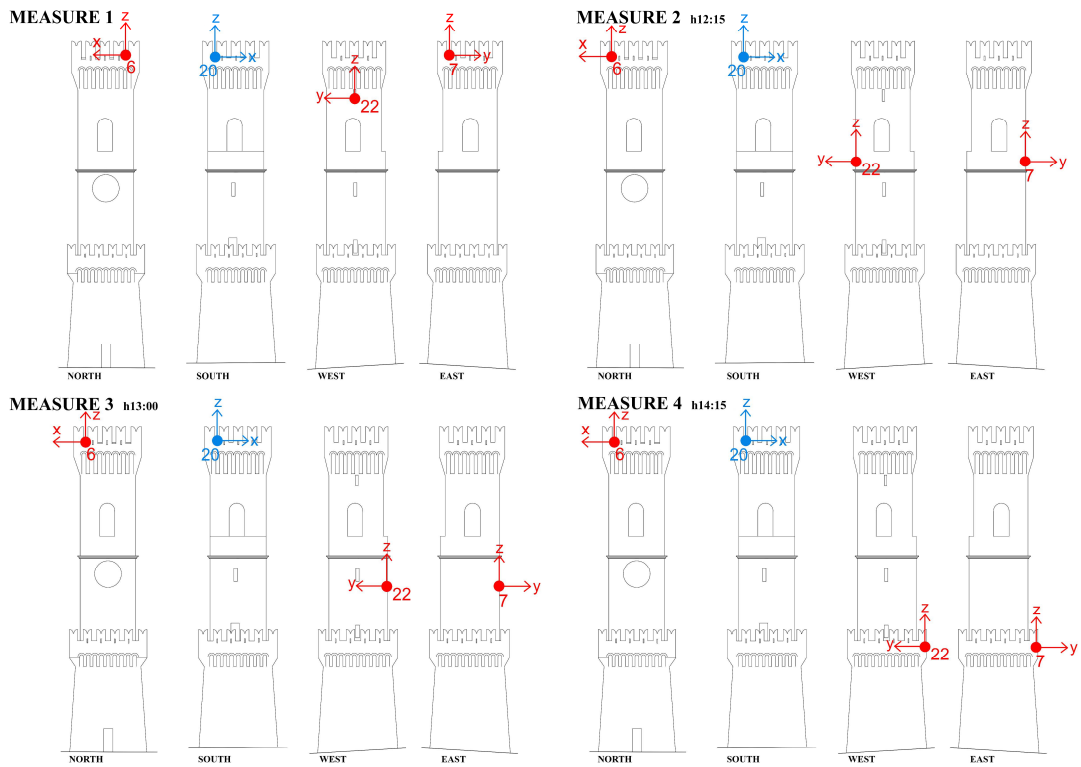
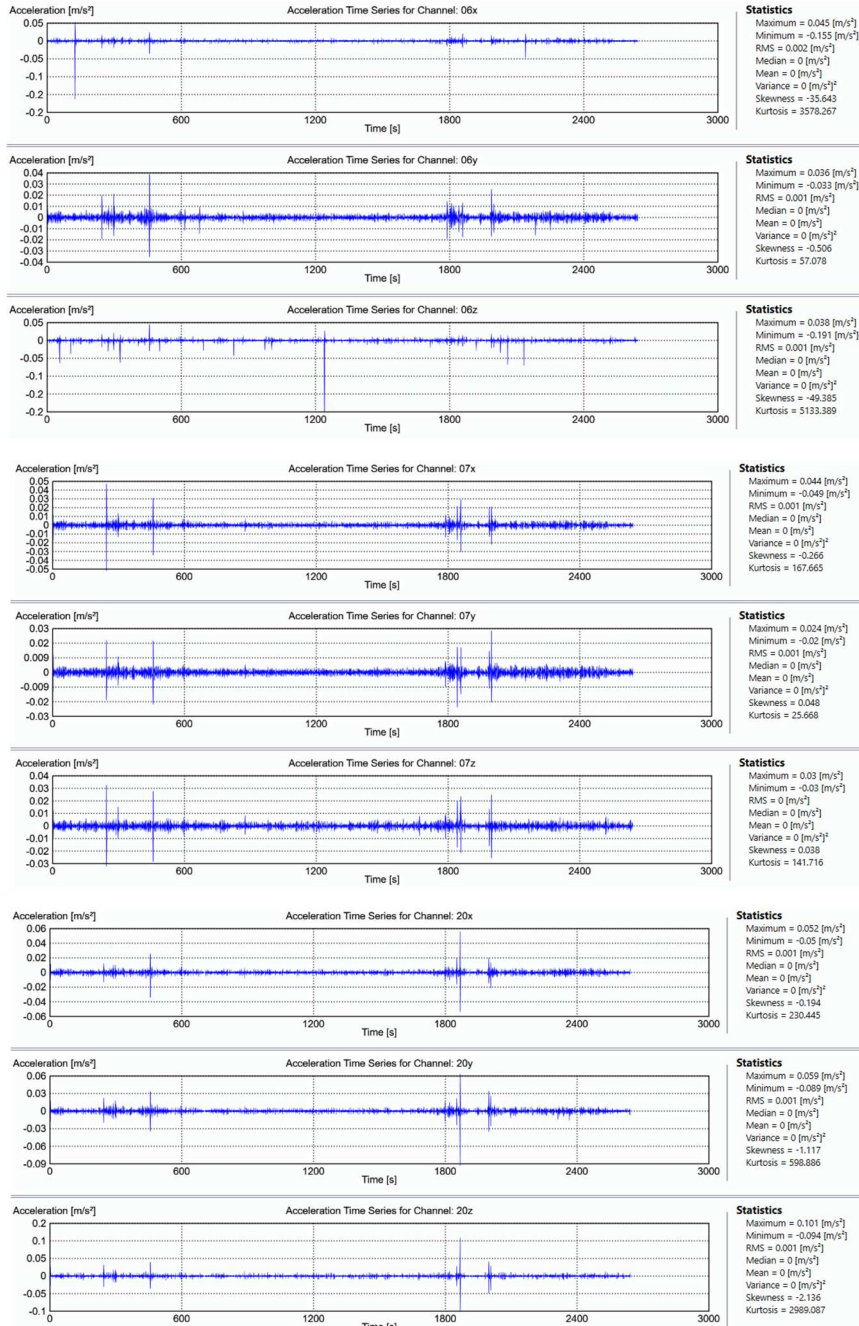
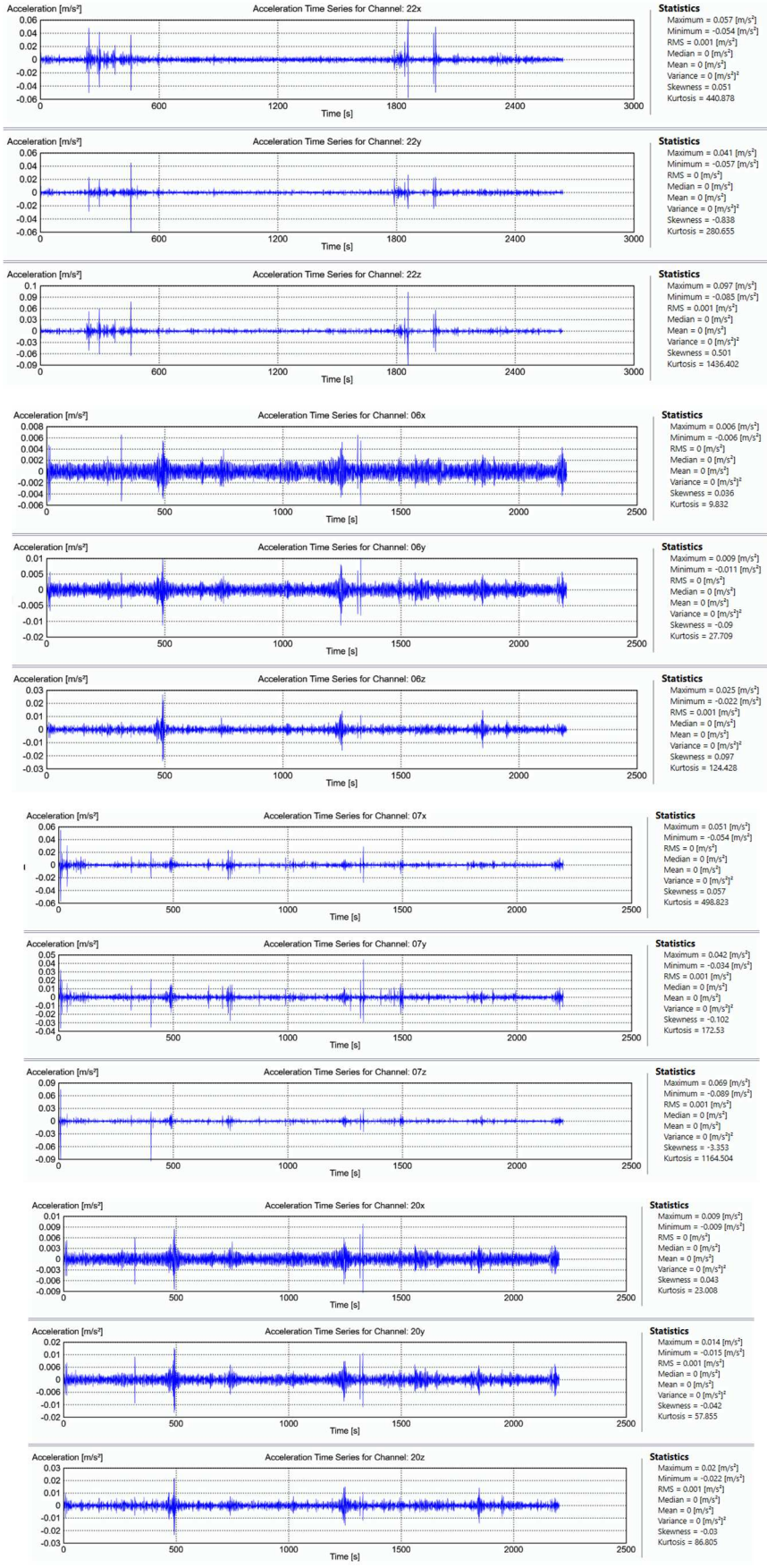


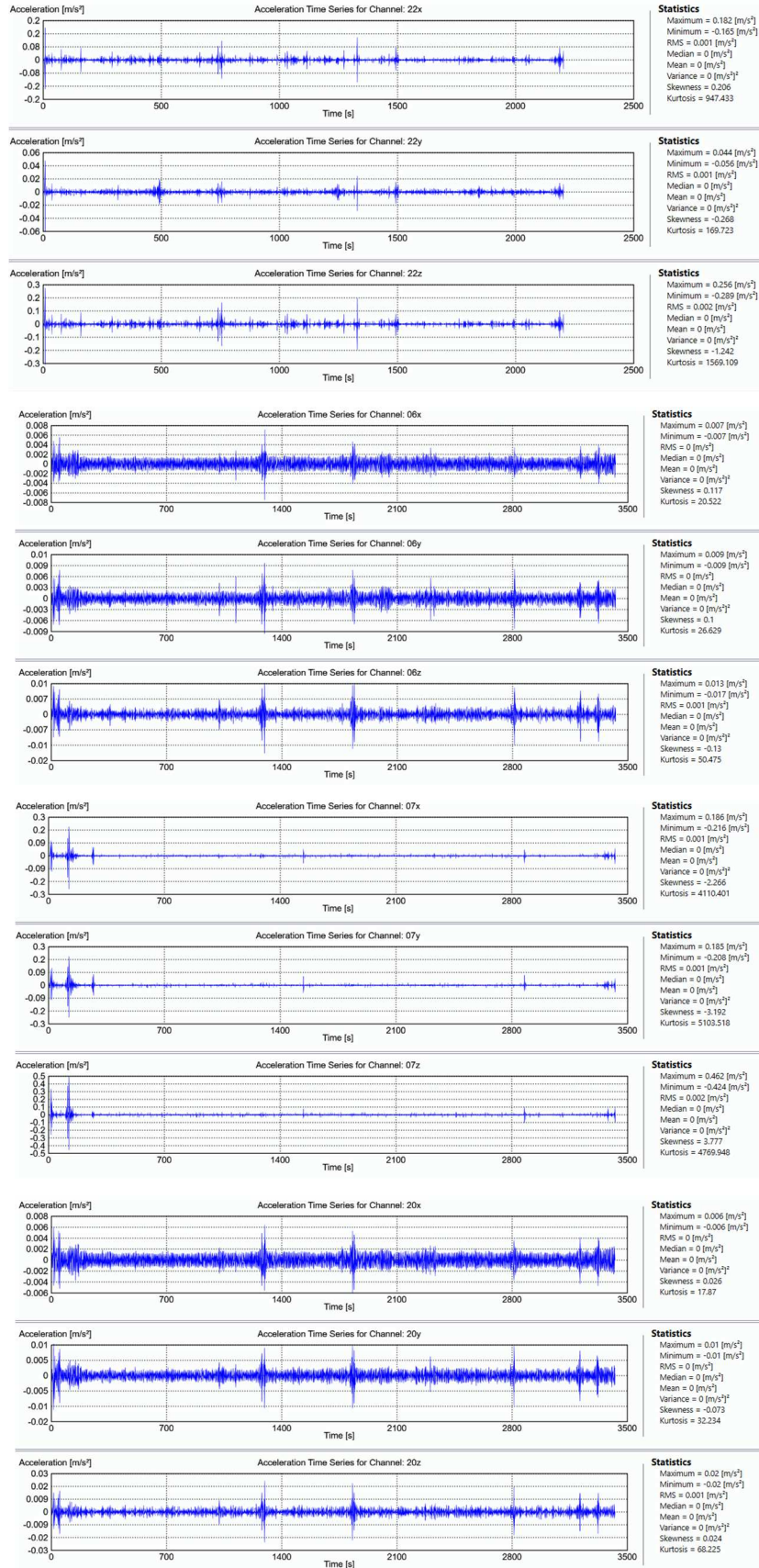
Figure 3-4 – Sensor positions in elevation

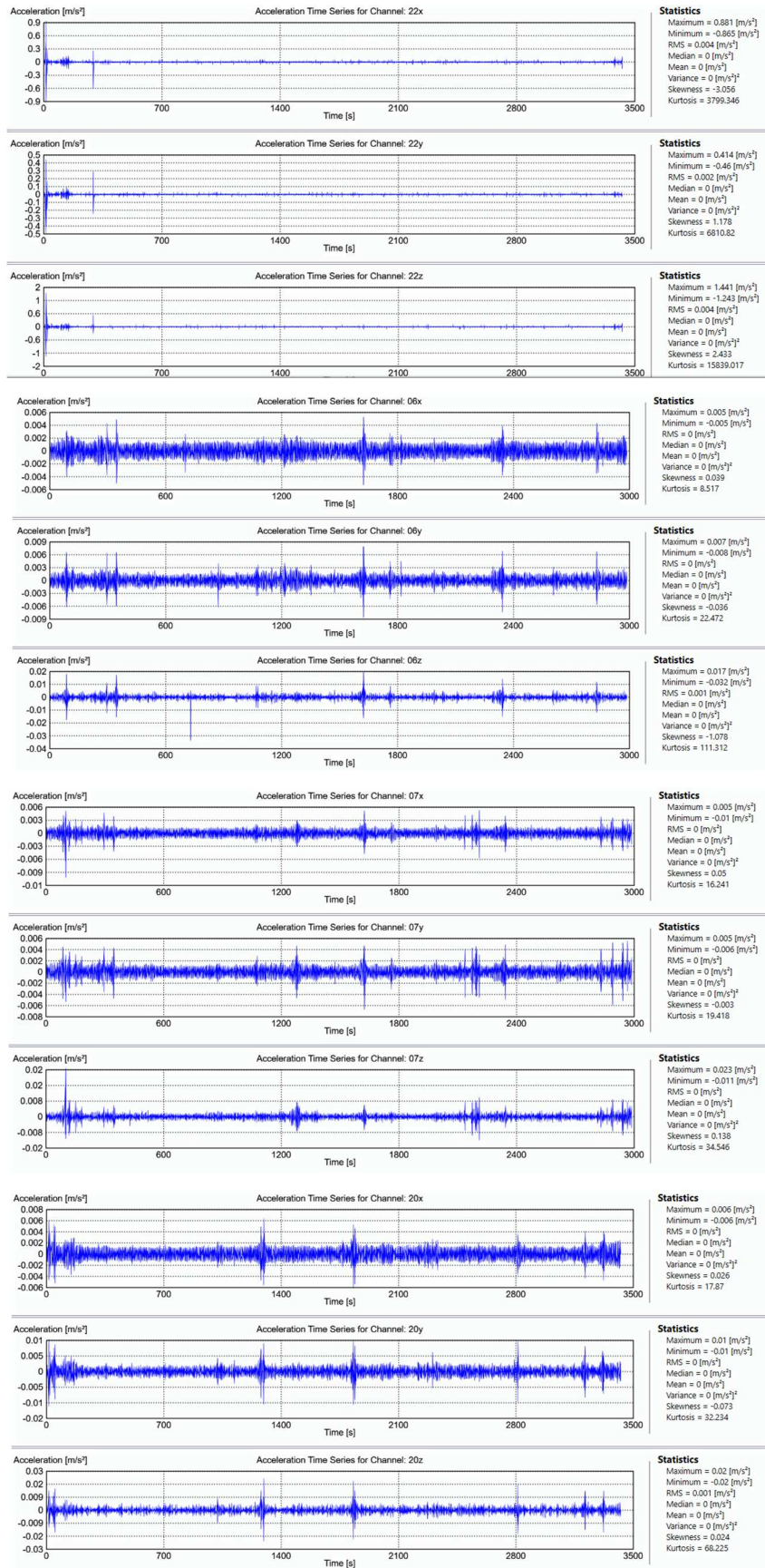
3.2.2.3 Experimental results

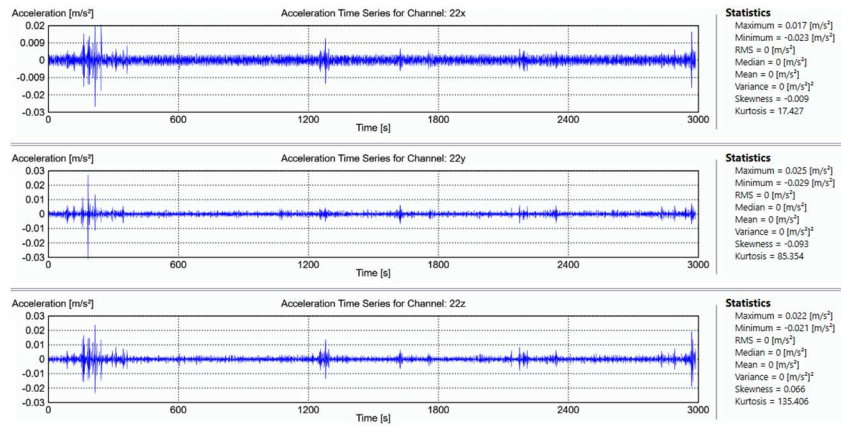
The signals obtained by the measurements of the first monitoring survey (June 29th, 2018) are shown in the following Figure. The figures report for each sensor the acceleration (m/s^2), as a function of time (s), along the three axes X,Y,Z.



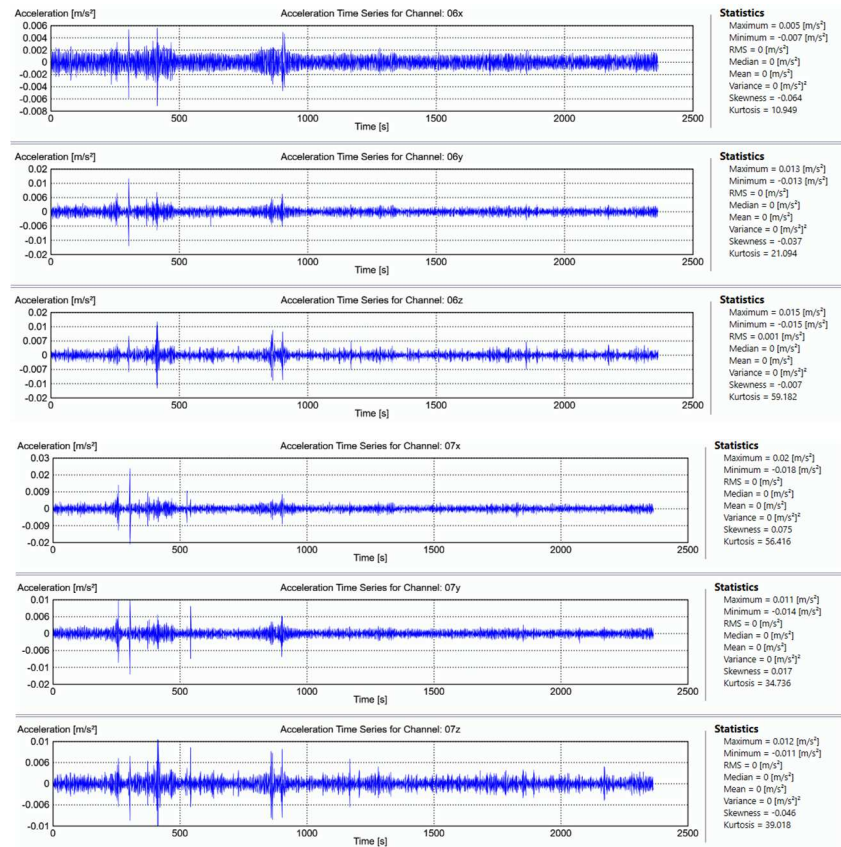


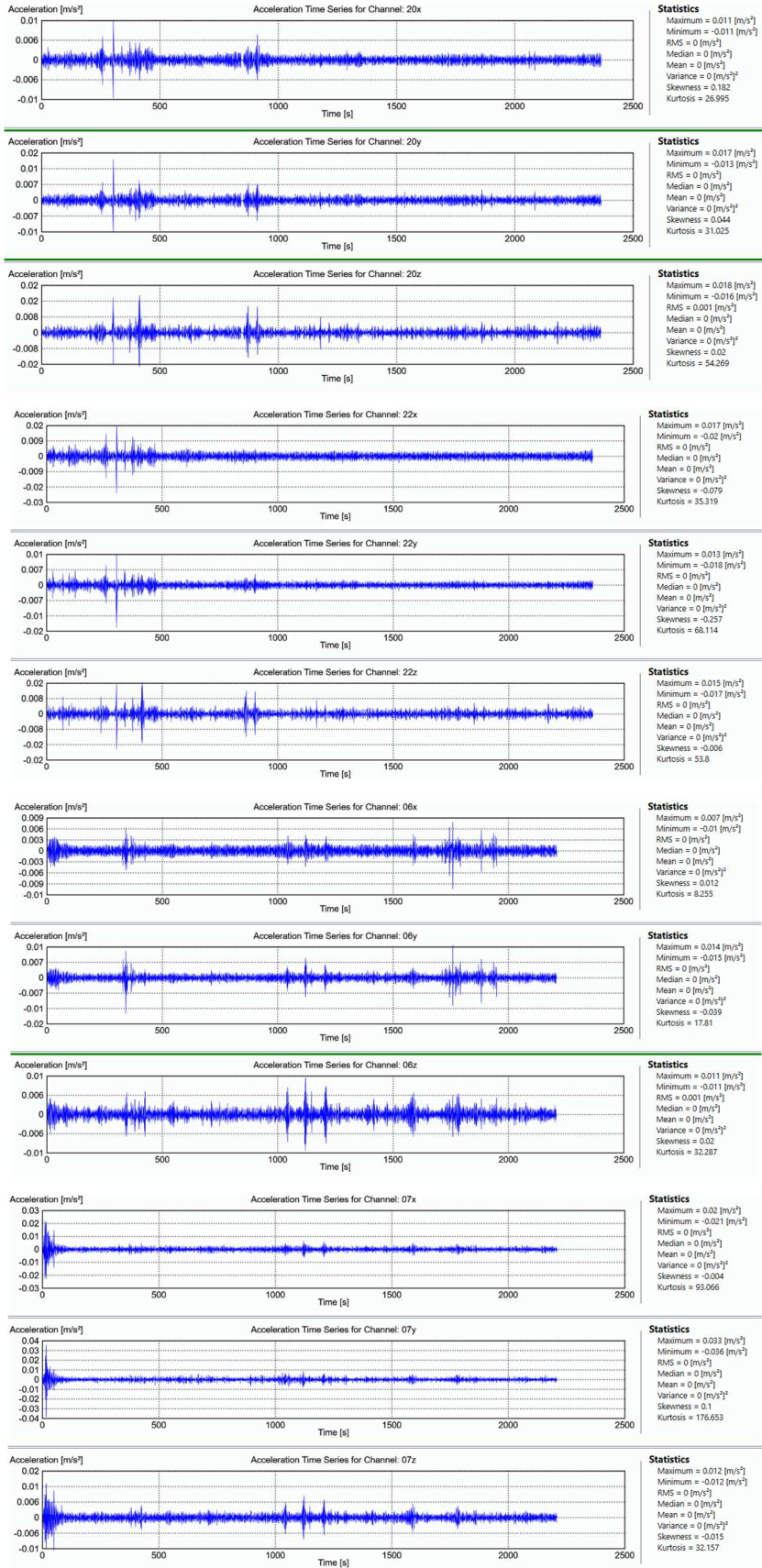


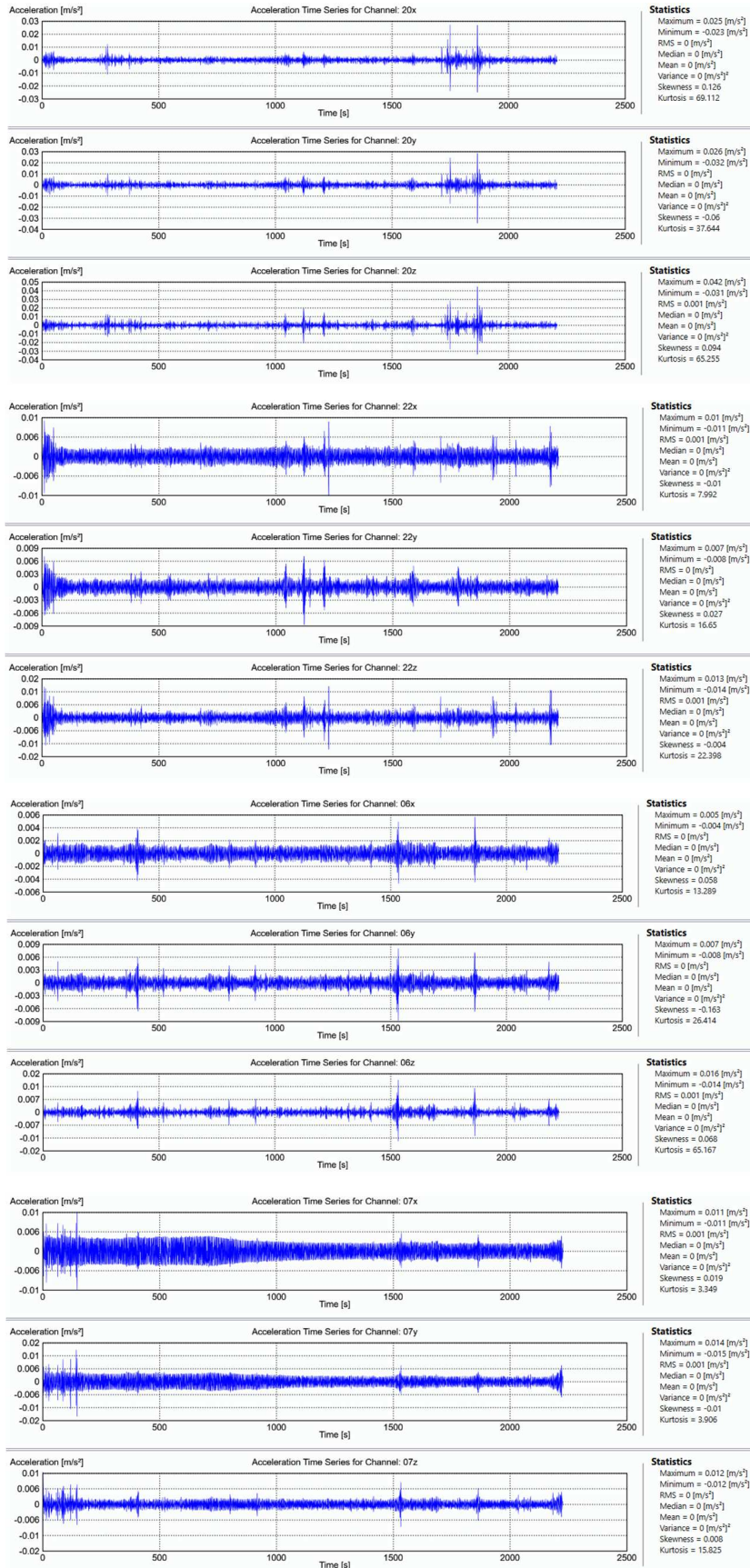


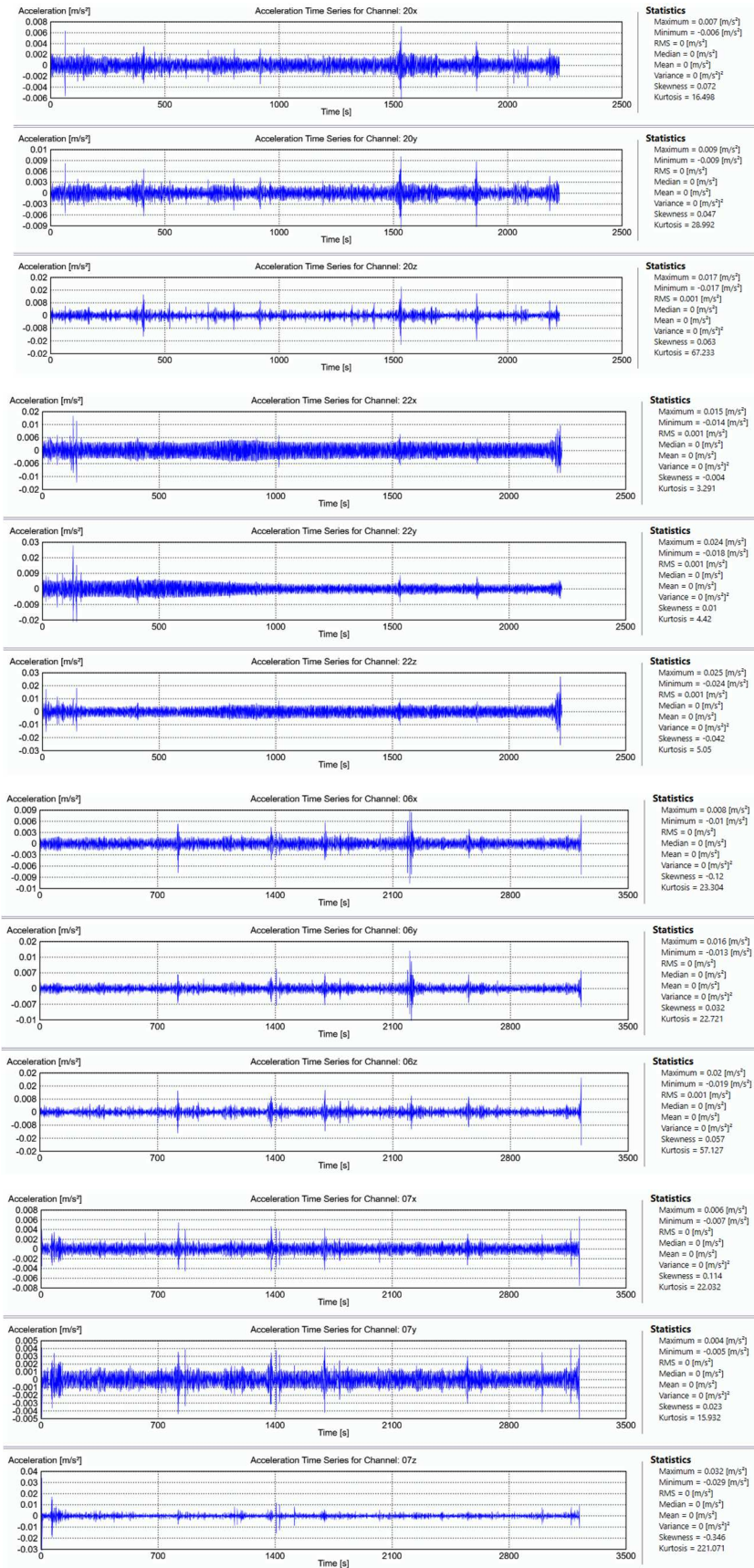


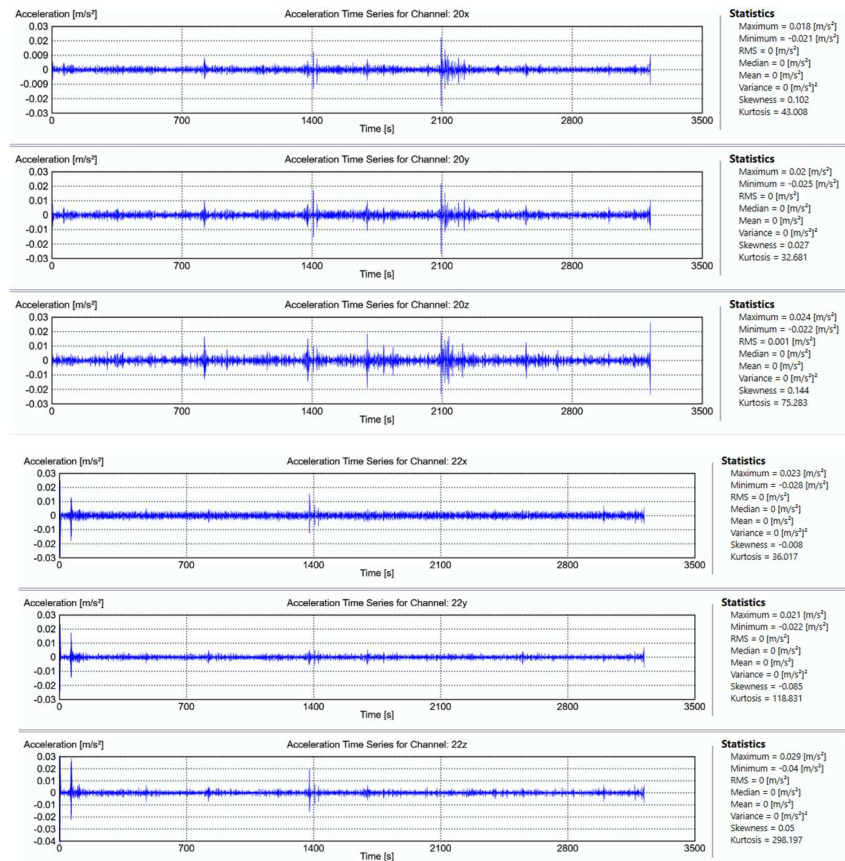
The signals of the measurements of the second monitoring survey are shown in the Figure below.











3.2.3 Modal parameters estimation using Artemis modal pro software

The modal identification of the examined structure, subjected to an environmental excitation, through the Ambient Vibration Testing technique described in previous chapter, allowed obtaining important modal parameters such as the structure vibration modes, the natural frequencies and the coefficients damping of the same.

The collected data were implemented on the ARTeMIS Modal Pro software in order to obtain the results mentioned above. ARTeMIS Modal is a powerful and versatile tool designed for modal testing, modal analysis and modal problem solving. Measuring the vibrations, ARTeMIS Modal can give you the modes in terms of mode shape, natural frequency and damping ratio. For two decades ARTeMIS Modal has been the preferred software for Operational Modal Analysis (OMA).

First of all, the geometry of the structure has been defined consisting of a set of points (from 1 to 87), appropriately referring to the coordinate system defined in the model, of horizontal and vertical lines joining the various points and therefore of surfaces enclosed

by lines. The geometry thus elaborated has the sole purpose of defining the position of the accelerometers on the structure and of evaluating the overall behaviour, while no definition of wall thicknesses or material characteristics is required.

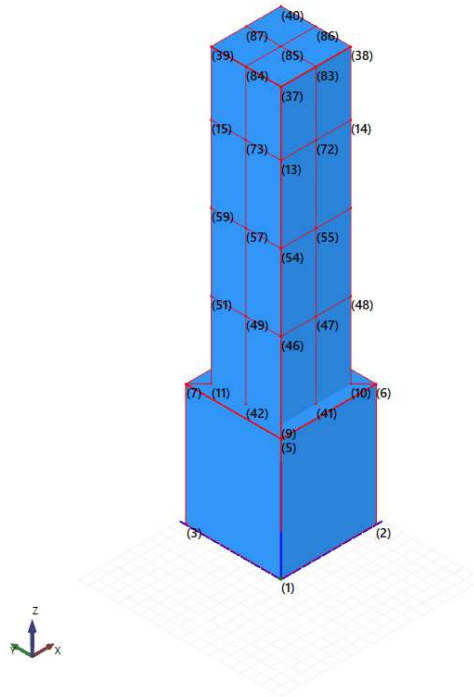


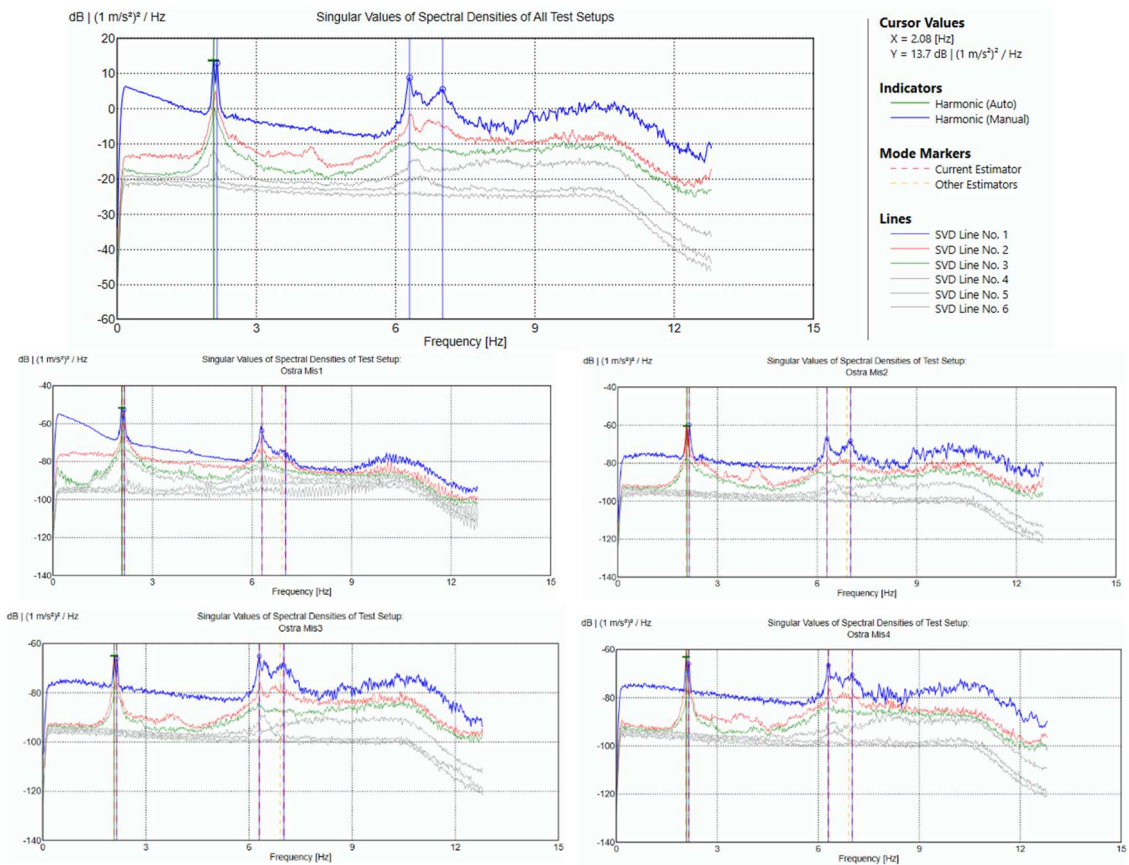
Figure 3-5 – Geometry of the tower

The next step was to load the recordings, organized in the different setups, and assign a degree of freedom (DOF) to each sensor in the three directions.

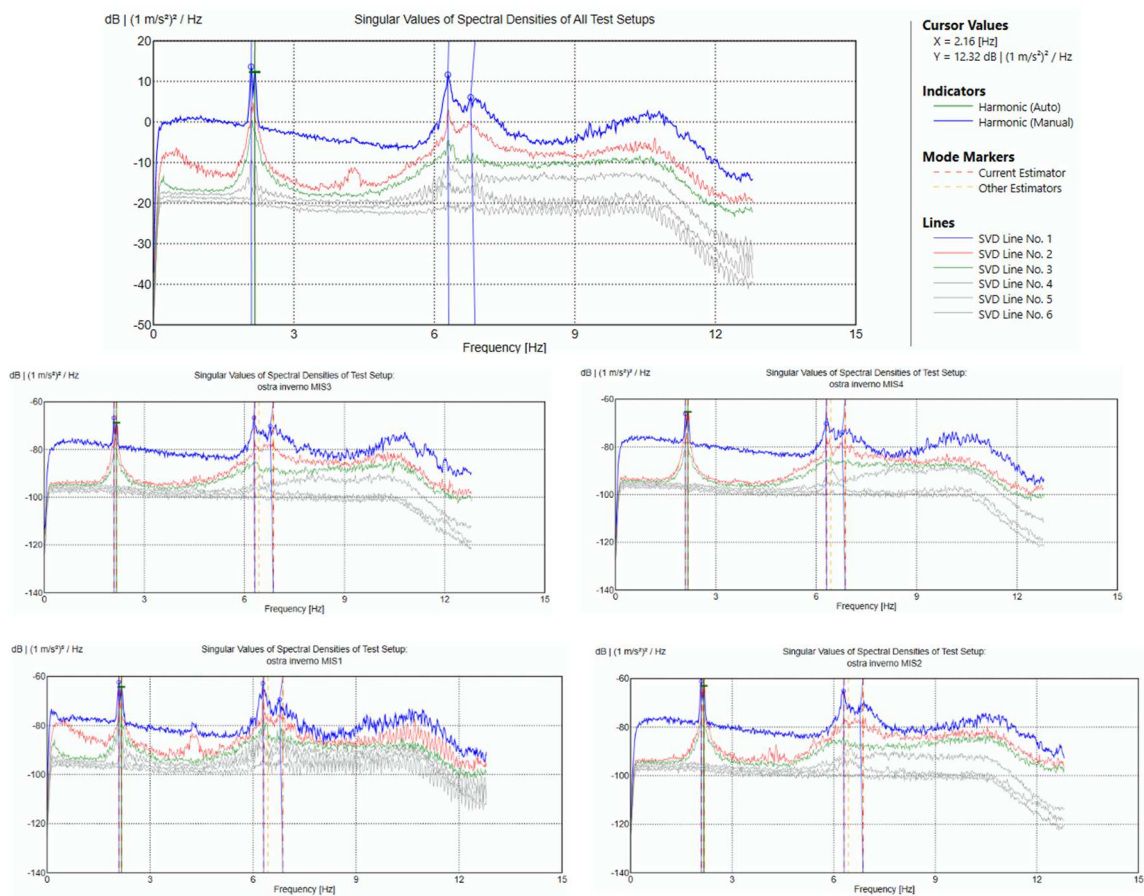
Once geometry and measurements are put together, everything is ready to start processing the measurements in the various ways needed in order to perform modal analysis.

A decimation of the signal was made and the new frequency range selected was 0 – 12.8 Hz. The purpose of decimation is to reduce the frequency range to the frequency range of interest. If you want to work in the frequency domain, it is desirable to decimate to zoom to the range of interest. If you are working with parametric models in the time domain, you should decimate in order to introduce poles only in the frequency range of interest. The decimation is basically a process where some samples are discarded and some samples are kept. However, in order to prevent aliasing, the signal is first low-pass filtered and then the excessive samples are discarded. The frequency Resolution of the spectral density diagrams was set at 1024 Hz.

The results of the modal analysis are shown in the Figures below. The first Operational Modal Analysis estimator selected is the Enhanced Frequency Domain Decomposition (EFDD). The frequencies are picked by the peak picking technique.



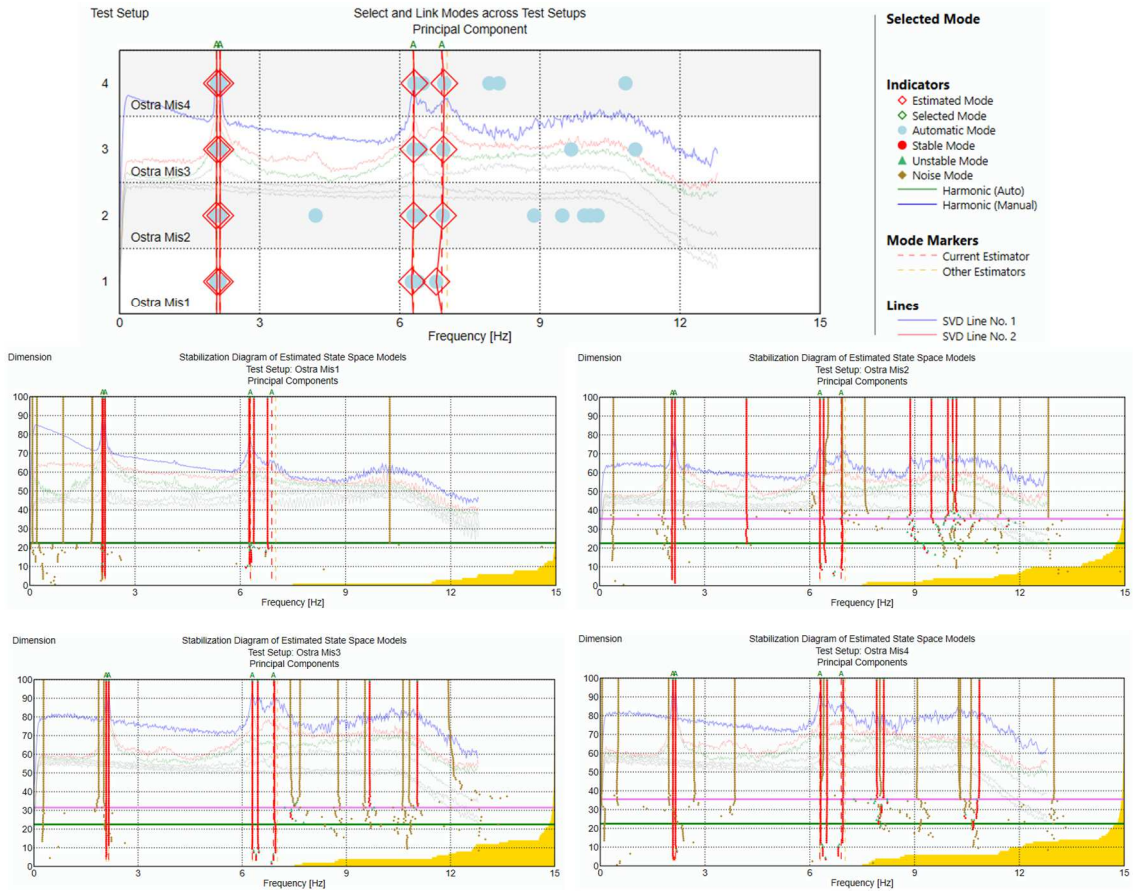
(a)



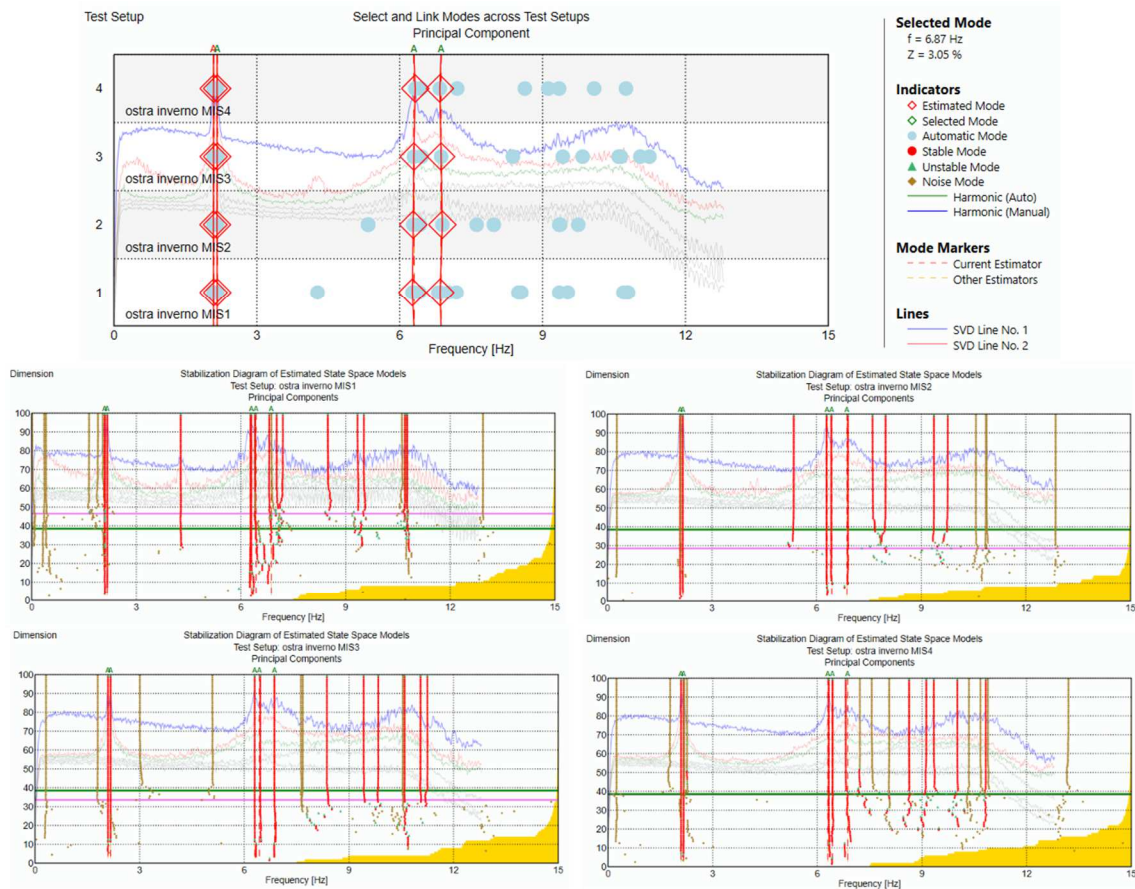
(b)

Figure 3-6 – (a) Diagrams of the EFDD analysis for the first monitoring survey. (b) Diagrams of the EFDD analysis for the second monitoring survey. In the two figures (a) and (b), the first diagram combines the results of all setups, while the others refer to the singular setup. The vertical lines identify the peaks of the spectrum, i.e. the fundamental frequencies, while the coloured lines display the singular values the estimated spectral density matrix. At each frequency there are as many singular values as the measurement channels in the currently selected test setup.

The second selected OMA estimator is the Stochastic Subspace Identification Principal Component (SSI-PC). The results of this analysis are shown in the following Figure.



(c)



(d)

Figure 3-7 - (a) Diagrams of the SSI-PC analysis for the first monitoring survey. (b) Diagrams of the SSI-PC analysis for the second monitoring survey. The first diagram represents all the test setups, while the others are the diagrams of the singular setup. The red dots correspond to the stable poles of the stabilization diagram, which comes out analysing in an iterative way the temporal signals that are acquired during the identification. In an iterative way, there is the estimation of frequencies, damping and modal forms

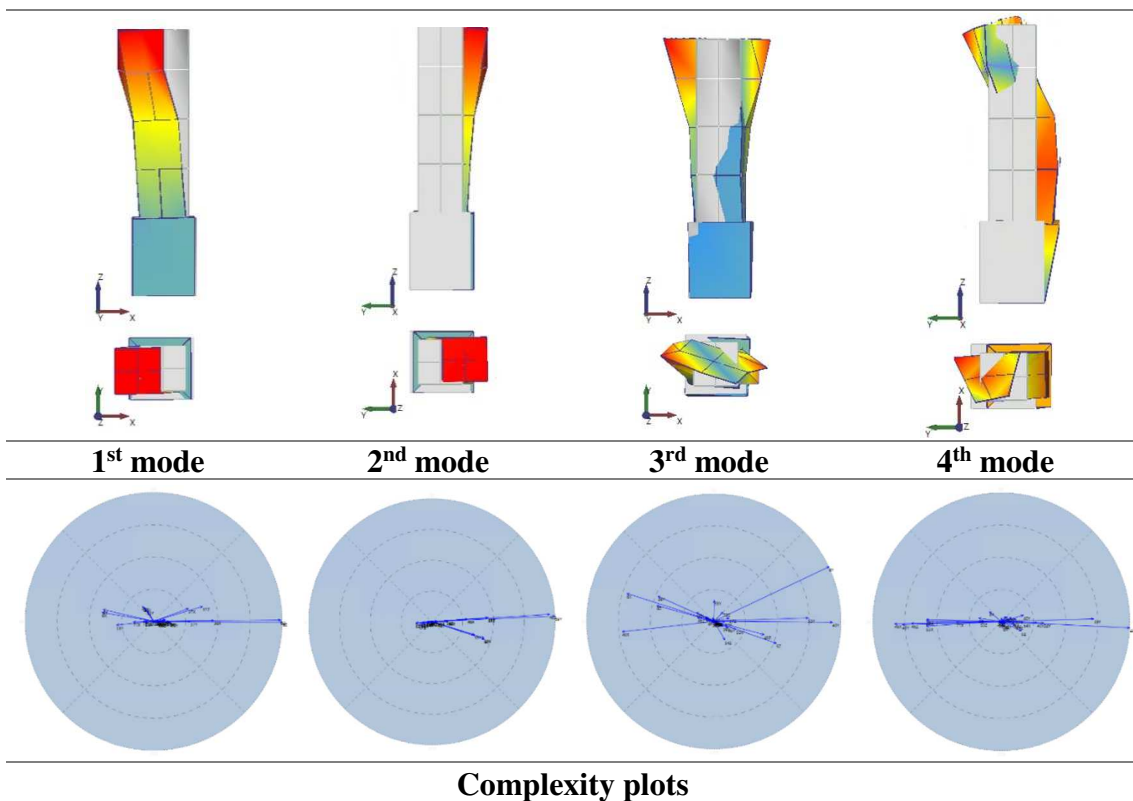
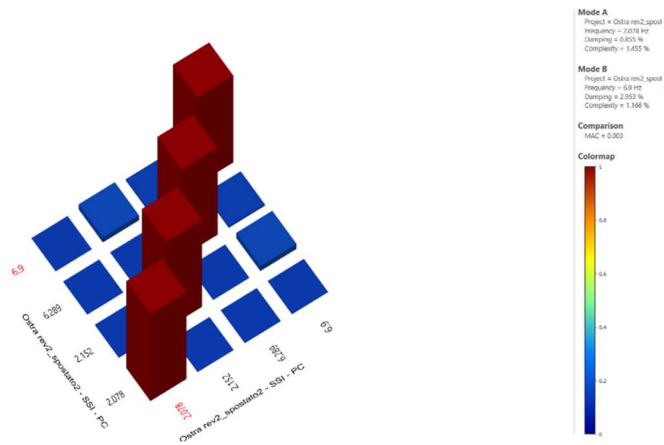
The validation of the time domain estimation of the state space models is actually performed in frequency domain. The reason for this is that it is very easy in frequency domain to see the repeated trend of structural modes when estimating multiple state space models. But the actual estimation is performed on the raw time series data of the currently selected test setup in time domain. The stabilization diagram presents the natural frequencies of all the estimated eigenvalues as well as a background wall-paper of the

Singular Value Decomposition of the spectral density matrices of the currently selected test setup.

The final chosen estimator was the SSI-PC, so the results in terms of frequencies and mode shapes, obtained with this method, are illustrated in the following pages, where the first Table reports the mode number, the type of mode shape, the natural frequency (Hz) and the damping ratio (%); the following pictures represent the MAC diagram (see Chapter 4, paragraph 4.2.5.1 for MAC explanation), the mode shapes in planar and elevation view and the complexity plots.

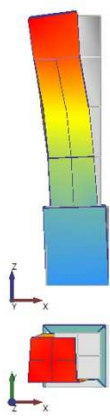
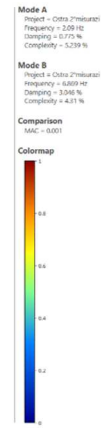
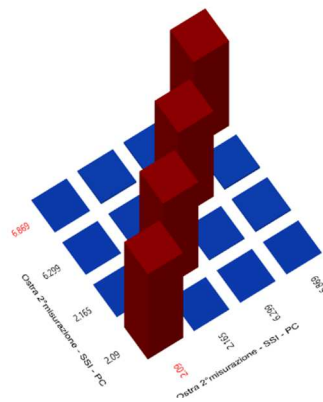
The results of the first monitoring survey are:

Mode number	Type	Natural frequency (Hz)	Damping ratio (%)
1	Translational X	2.087	0.855
2	Translational Y	2.152	0.851
3	Torsional Z	6.289	0.655
4	Bending Y	6.900	2.953

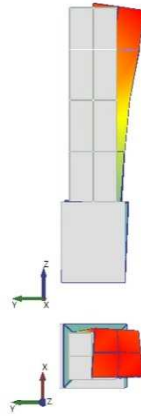


The results of the second monitoring survey are:

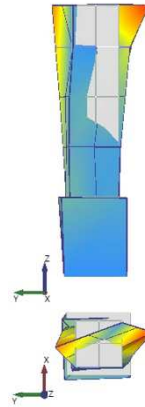
Mode number	Type	Natural frequency (Hz)	Damping ratio (%)
1	Translational X	2.090	0.755
2	Translational Y	2.165	0.754
3	Torsional Z	6.299	0.710
4	Bending Y	6.869	3.046



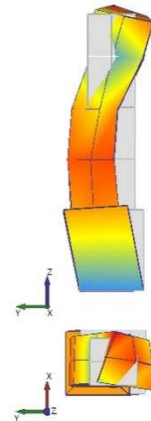
1st mode



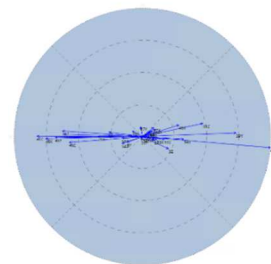
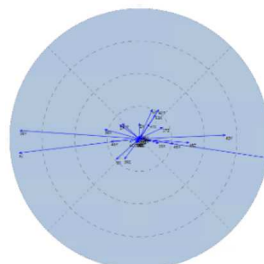
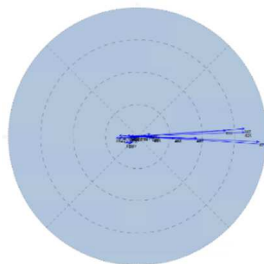
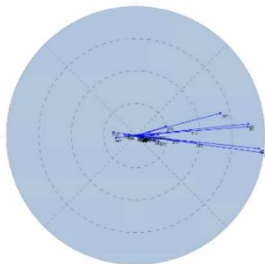
2nd mode



3rd mode



4th mode



Complexity plots

The identified frequencies appear rather spaced. The first two mode are translational modes; the torsional component is visible with the 3rd mode that always involves the tower in the upper part. The 4th mode involves the top and the second floor and it is a bending mode.

Complexity plots may also be very useful to check if the shapes are normal or not.

Modes can be divided into two types, normal modes and complex modes. The mode shape of normal modes can be described as a sign valued real number. The mode shape of complex modes is complex valued and cannot be described as a real number. In other words, with normal mode, all DOF points of the structure are moving in phase or 180 degree out of phase with each other. With complex mode, the different DOF points of the structure are moving in some general phase relationship with each other. The damping property of a structure decides whether the modes will be normal or complex. For lightly or proportionally damped structures, the estimated modes should approximate normal. In practice, the normal modes on the structure could be estimated as complex modes due to the distorted FRF measurements, curve fitting error or some other inaccuracies.

If the component is real valued, the arrows in the complexity plot point in an horizontal direction, so complexity is illustrated by the vertical component. In ARTeMIS Modal it is the normalized mode shape that is displayed.

The third mode, as can be seen in the results of both monitoring surveys, has a high complex part: this will lead to some difficulties in the calibration of the numerical model, as explained in Chapter 4.

It can be affirmed that the frequencies obtained in the second monitoring survey are almost equal to those obtained in the first survey. The structure didn't suffer from further structural damage during the period between June 2018 and February 2019. Not even the temperature change seems to have affected the tower behaviour.

3.3 A comparison between two softwares for OMA: ARTeMIS and ModalVIEW

ModalVIEW is another software, as ARTeMIS Modal Pro, designed to acquire multi-channel vibration signals from static or dynamic loading of a structure by utilizing data acquisition hardware. After obtaining a set of time histories, it can show the response of a structure and its vibration behaviour. It extracts and visualizes modal parameters information from acquired time- and frequency-domain experimental data. Natural frequencies, damping ratios and mode shapes are extracted by a series of modal analysis methods to analyse dynamic behaviour of the structures.

As in ARTeMIS Modal Pro software, the geometry can be easily drawn by points, lines and surfaces.

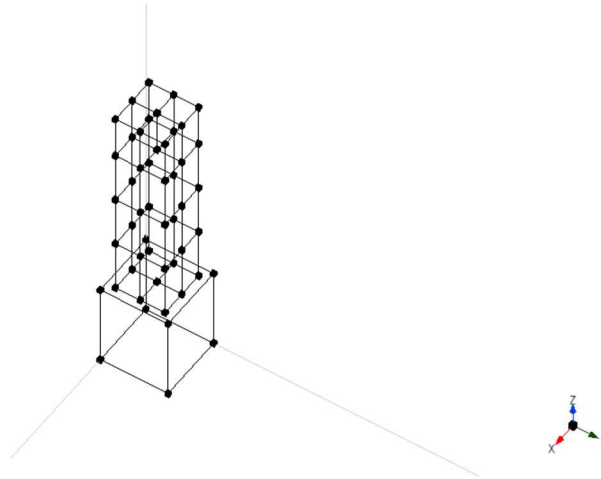


Figure 3-8 – Geometry of the model

Each node on 3D model has a local coordination. The X, Y, Z axes of local coordination defines three measurement directions. There are three measure types defined for the measurement directions of each node on 3D model: Measured, Interpolated and Fixed. Measured nodes on 3D model correspond to the measurement points on physical object, where measurements are actually made. There are much more nodes used to create 3D model structure than the number of actually measured points, where the sensors are fixed on. Interpolated and fixed nodes are the nodes that don't have a corresponding measurement data with them. During structure animation, the motion of measured nodes is determined by assigned measurement data. The motion of interpolated nodes is

computed according to the motion of neighbouring measured nodes. The fixed nodes are not animated.

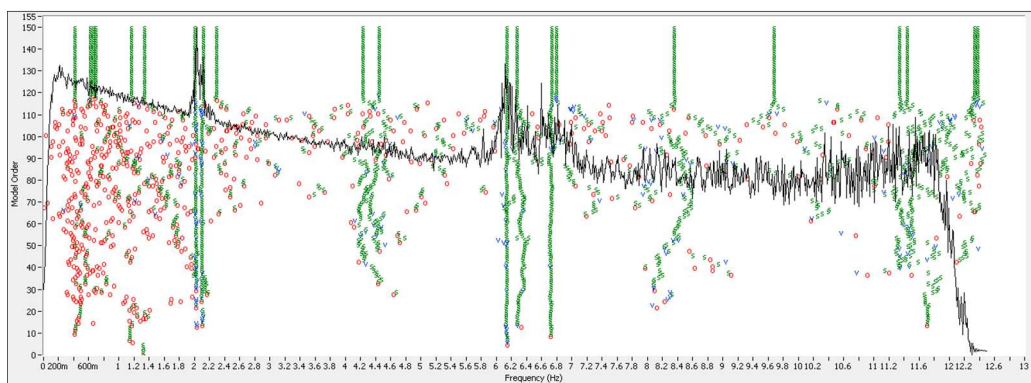
As both measurements (June 2018 and February 2019), analysed in ARTeMIS, led to the same results, only the measurement of June was implemented in ModalVIEW.

After importing the data relating to the individual channels, they must be decimated obtaining a sampling frequency of 12.5Hz.

For the determination of modal parameters, the first step is to define the parameters to generate the diagram of stabilization. The valid modal forms are identified in this diagram, which shows the stable poles depending on the model order and considering only the modal forms with a damping of less than 15%. It is necessary to set SSI method and model order equal to 150; the frequency is considered stable if it has no variation greater than 2%, the damping equal to 15%. The mode shape with a certain order is compared with the same obtained with a minor order through the Modal Assurance Criterion (MAC), which must be at least equal to 90%. The extraction of the modes is carried out automatically by the software, setting a frequency width equal to 0.1 and a number of stable modes equal to 20.

In ModalVIEW the measurement setups are analysed singularly and there isn't the possibility, contrary to ARTeMIS, to have a result diagram for all the setups.

Figure 3-9 reports the stabilization chart for each test setup.



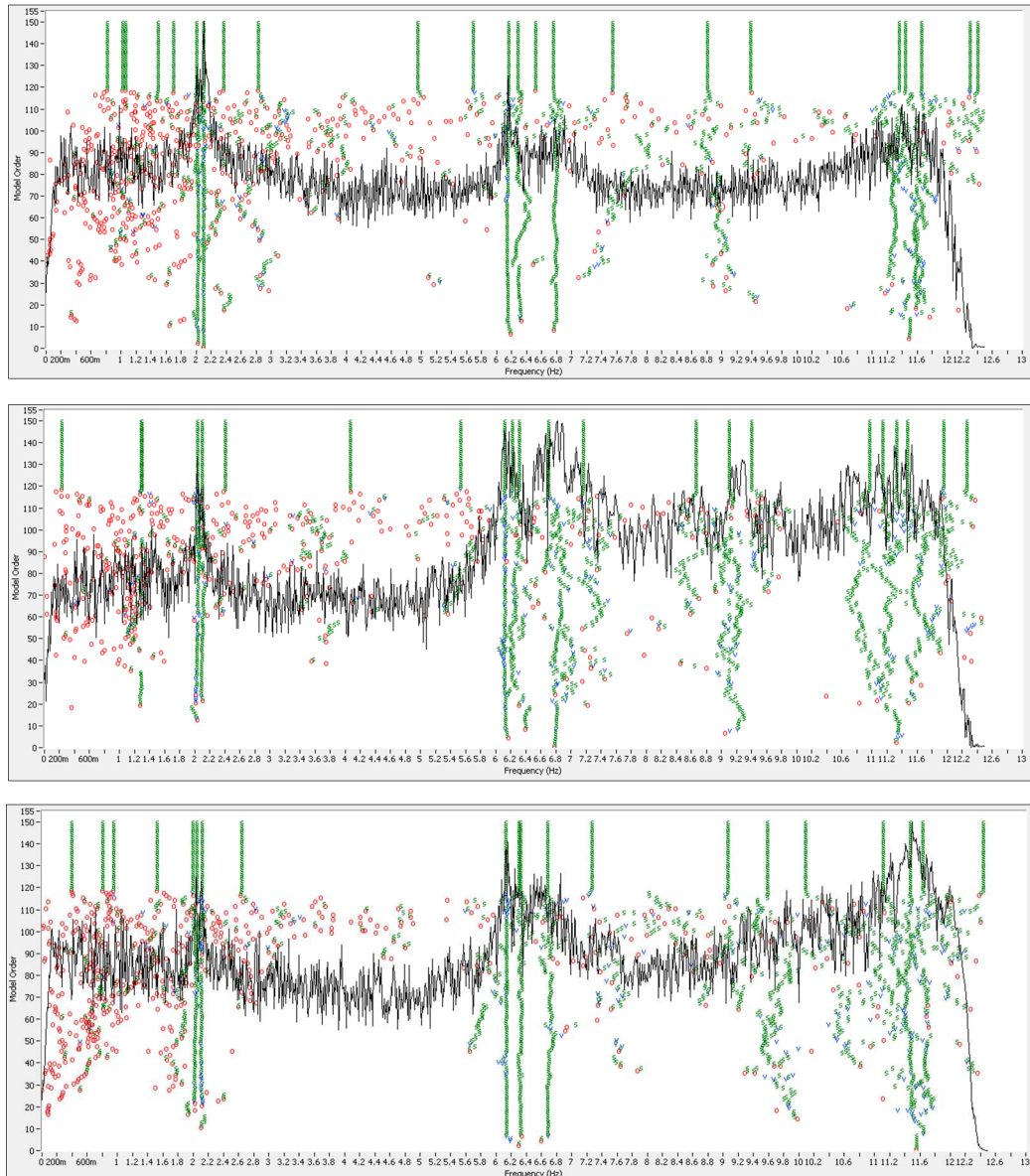


Figure 3-9 – Stabilization charts for each test setups

Stabilization chart is used to find physically meaningful modes from a set of computed modes by curve fitting. The stabilization chart is created with horizontal axis being frequency and vertical axis being model order. The computed modes for a range of model orders (number of modes to estimate) are displayed on the chart. Theoretically, the physical modes of the structure always appear at a nearly identical frequency, this is an indication that physical modes are stable, while mathematical or fake modes scatter at different frequency. The mode stability is decided by the stability of its three modal parameters, frequency, damping and modal shape.

The stability criteria are defined as the changing ratio of modal parameters from a lower model order to a higher model order as following:

$$\frac{|p_n - p_{n-1}|}{p_{n-1}} \times 100\% \quad (19)$$

The typical values for stability criterion:

- Frequency stability
- Damping ratio stability
- Modal shape stability

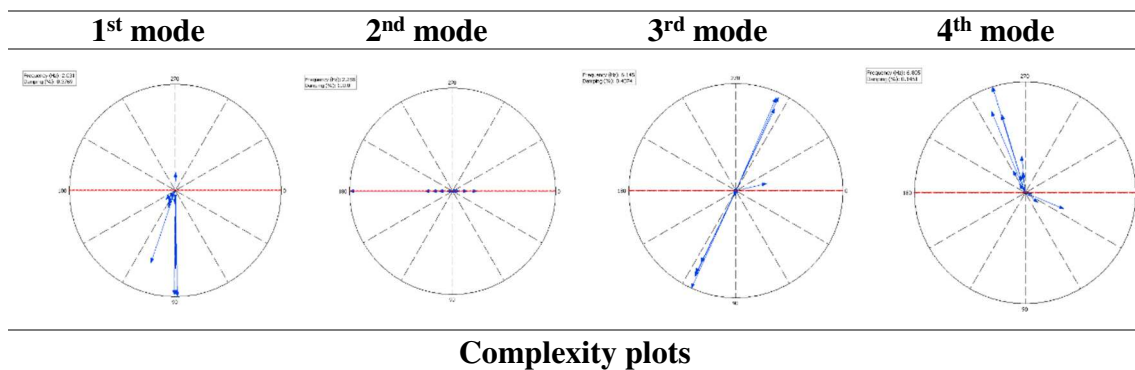
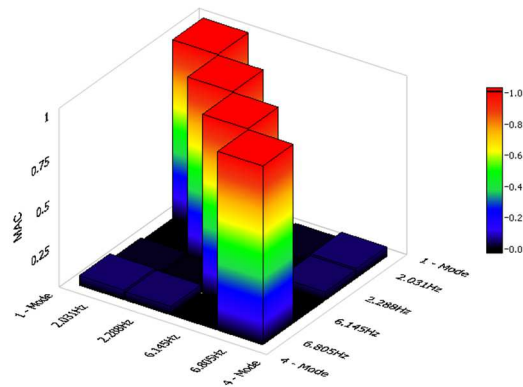
The computed modes on stabilization chart are represented using a group of symbols, s, v, d, f and o. Each symbol represents an estimated mode. The symbols indicate if the estimated mode is stable or not (Table 3-1)

Symbol	Frequency	Damping ratio	Mode shape
s	yes	yes	yes
v	yes	no	yes
d	yes	yes	no
f	yes	no	no
o	no	no	no

Table 3-1

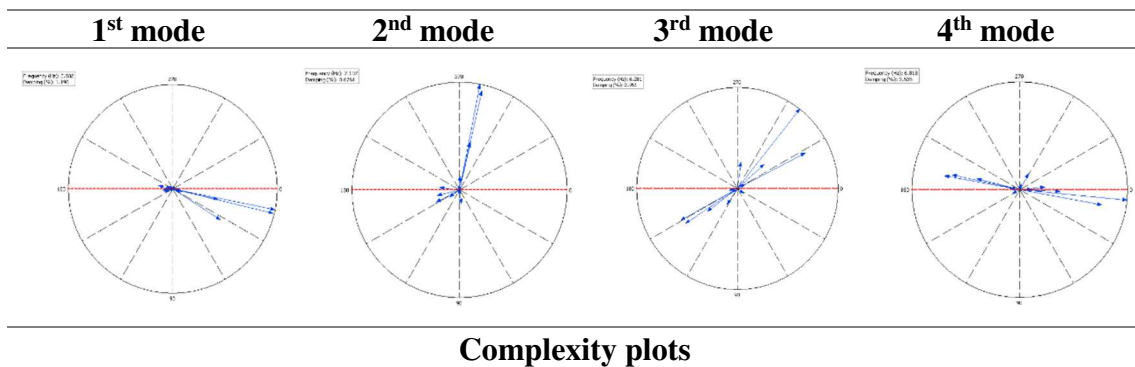
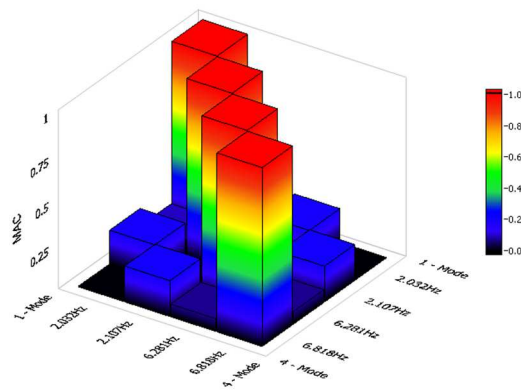
Results of the first setup:

Mode number	Natural frequency (Hz)	Damping ratio (%)
1	2.031	0.377
2	2.288	0.754
3	6.145	0.407
4	6.805	0.145



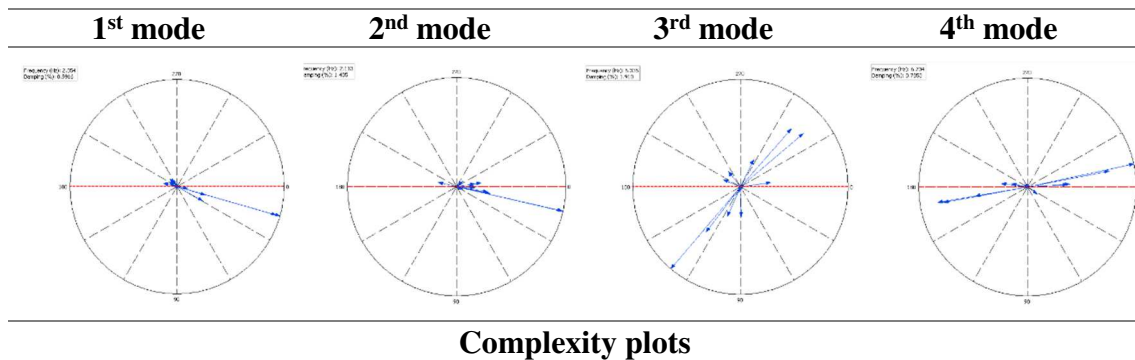
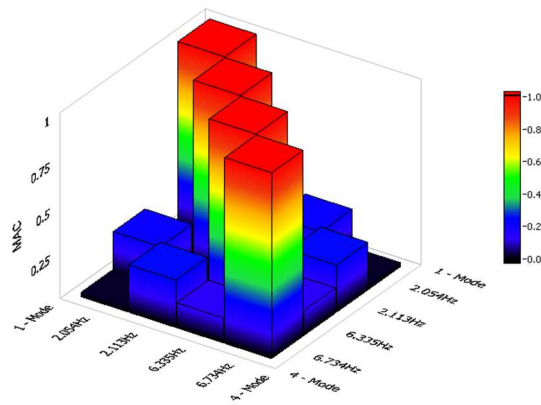
Results of the second setup:

Mode number	Natural frequency (Hz)	Damping ratio (%)
1	2.032	1.190
2	2.107	0.676
3	6.281	2.951
4	6.818	3.535



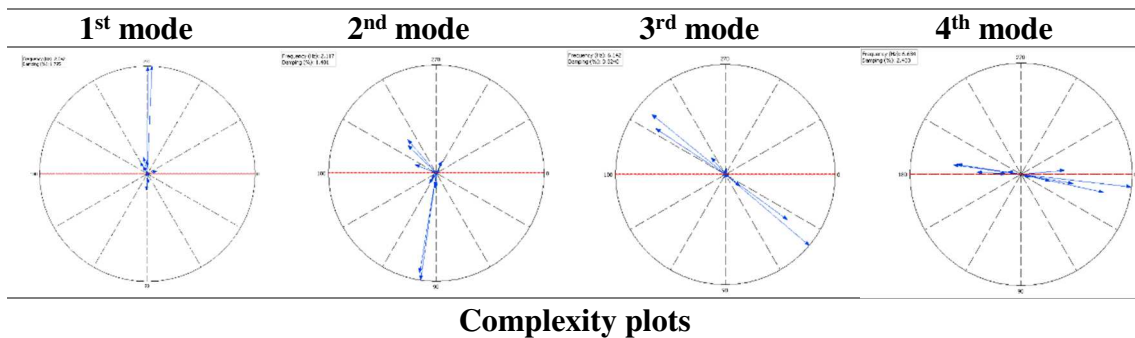
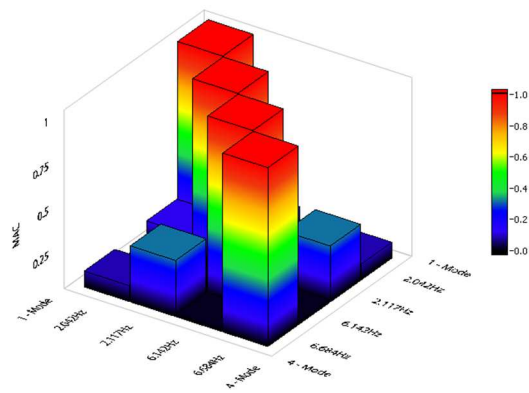
Results of the third setup:

Mode number	Natural frequency (Hz)	Damping ratio (%)
1	2.054	0.992
2	2.113	1.485
3	6.335	1.910
4	6.734	0.785



Results of the fourth setup:

Mode number	Natural frequency (Hz)	Damping ratio (%)
1	2.042	1.795
2	2.117	1.401
3	6.142	0.324
4	6.684	2.433



The results of the four setups are similar to that of ARTEMIS. The natural frequencies estimated are almost equal compared to each other and to that obtained in the previous chapter.

Chapter 4

Finite element modelling of the tower

4.1 Initial numerical model of the tower

A 3D FE model of the tower was built in FX+ for DIANA software, an additional pre/post-processor to DIANA with a user-friendly graphical user interface that enables to build complex models rapidly and accurately.

The geometry of the model was based on the results of the geometrical survey.

To create the structure, the first step was importing the plans of the tower previously drawn in Autocad; then, using solid elements as boxes or wedges, the model was constructed creating one floor at a time.

It is important to orient the model as the one in Artemis in order to easily compare them. An edge of the base coincides with the origin of the axes.

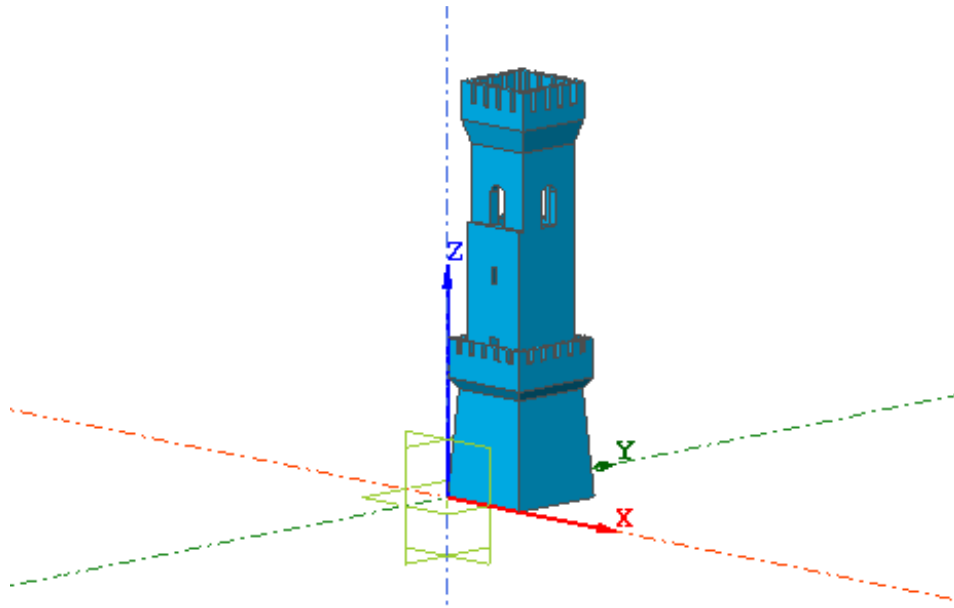


Figure 4-1 – Geometry of the model and work-plane

This initial model was composed of 7 solids.

Another fundamental operation is the “Boolean cut”: through this operation, two solids touching each other become congruent, while remaining distinct in their entity. The faces of the solids must fit together before the meshing operation.

The second step was the definition of the materials to apply to the model. Materials were identified according to the inspection work: masonry for the walls, concrete for the slabs and a filling of waste material for the rubble core of walls. All the materials were considered elastic and isotropic materials.

Initially the mechanical properties were estimated based on literature, such as the Italian regulations NTC2018 (table C8.5.I of Circolare esplicativa, see Table 4-1), or on experimental case for similar materials.

Tipologia di muratura	f_m (N/cm ²)	τ_0 (N/cm ²)	E (N/mm ²)	G (N/mm ²)	w (kN/m ³)
	Min-max	Min-max	Min-max	Min-max	
Muratura in pietrame disordinata (ciottoli, pietre erratiche e irregolari)	100 180	2,0 3,2	690 1050	230 350	19
Muratura a conci sbozzati, con paramento di limitato spessore e nucleo interno	200 300	3,5 5,1	1020 1440	340 480	20
Muratura in pietre a spacco con buona tessitura	260 380	5,6 7,4	1500 1980	500 660	21
Muratura a conci di pietra tenera (tufo, calcarenite, ecc.)	140 240	2,8 4,2	900 1260	300 420	16
Muratura a blocchi lapidei squadri	600 800	9,0 12,0	2400 3200	780 940	22
Muratura in mattoni pieni e malta di calce	240 400	6,0 9,2	1200 1800	400 600	18
Muratura in mattoni semipieni con malta cementizia (es.: doppio UNI foratura ≤ 40%)	500 800	24 32	3500 5600	875 1400	15
Muratura in blocchi laterizi semipieni (perc. foratura < 45%)	400 600	30,0 40,0	3600 5400	1080 1620	12
Muratura in blocchi laterizi semipieni, con giunti verticali a secco (perc. foratura < 45%)	300 400	10,0 13,0	2700 3600	810 1080	11
Muratura in blocchi di calcestruzzo o argilla espansa (perc. foratura tra 45% e 65%)	150 200	9,5 12,5	1200 1600	300 400	12
Muratura in blocchi di calcestruzzo semipieni (foratura < 45%)	300 440	18,0 24,0	2400 3520	600 880	14

Table 4-1 – Mechanical properties of some types of masonry (Italian regulation NTC2018)

Material	E (MPa)	ν	γ (kN/m ³)
masonry	1800	0.2	18
concrete	18000	0.2	25
filling	1100	0.2	18

Table 4-2 – Material properties of the initial model

For each material, it was defined the Young's modulus (N/m²), the Poisson's ratio and the mass density (N/m³/g).

Before the meshing operation, it is necessary to establish the type of element for the mesh and that was chosen in order to make the meshing process easier and to guarantee a great result and acceptable computational costs. The type of mesh chosen was TE12L element, a four-node, three-side isoparametric solid pyramid element; it is based on linear interpolation and numerical integration.

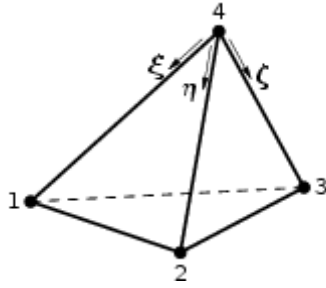


Figure 4-2 – Mesh element

It was also established the element size as 0.3m. After defining these parameters, an auto-mesh solid operation was performed. At the end of it, the model was perfectly meshed with every node connected to each other.

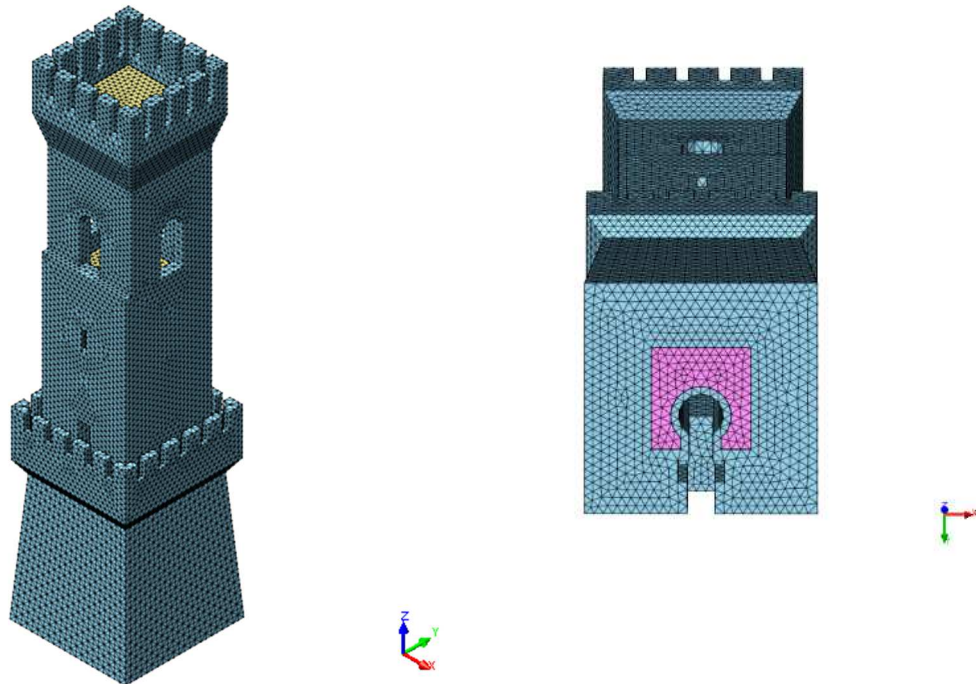


Figure 4-3 – Meshed model: the parts assigned to “masonry” material are in blue; in yellow, concrete slabs and columns. Lastly, the “filling” part is in violet

The meshed model had 38491 points and 172017 tetrahedral elements.

The last step was define the loads and the boundary conditions. Only gravitational loads were entered, like the body force, which represent the weight of the elements. As boundary conditions, all the nodes of the base were fixed, so no translations or rotations were permitted.

The model was saved in pre-natural format and imported in Diana software. An eigenvalue analysis was performed to know the modal parameters of the initial model of the tower. The eigenvalue analysis is a free-vibration analysis in which the stiffness and the mass are involved to determine the eigenfrequencies and to see the shape modes. The mode shapes of the numerical model obtained after the analysis are shown in Figure 4-4.

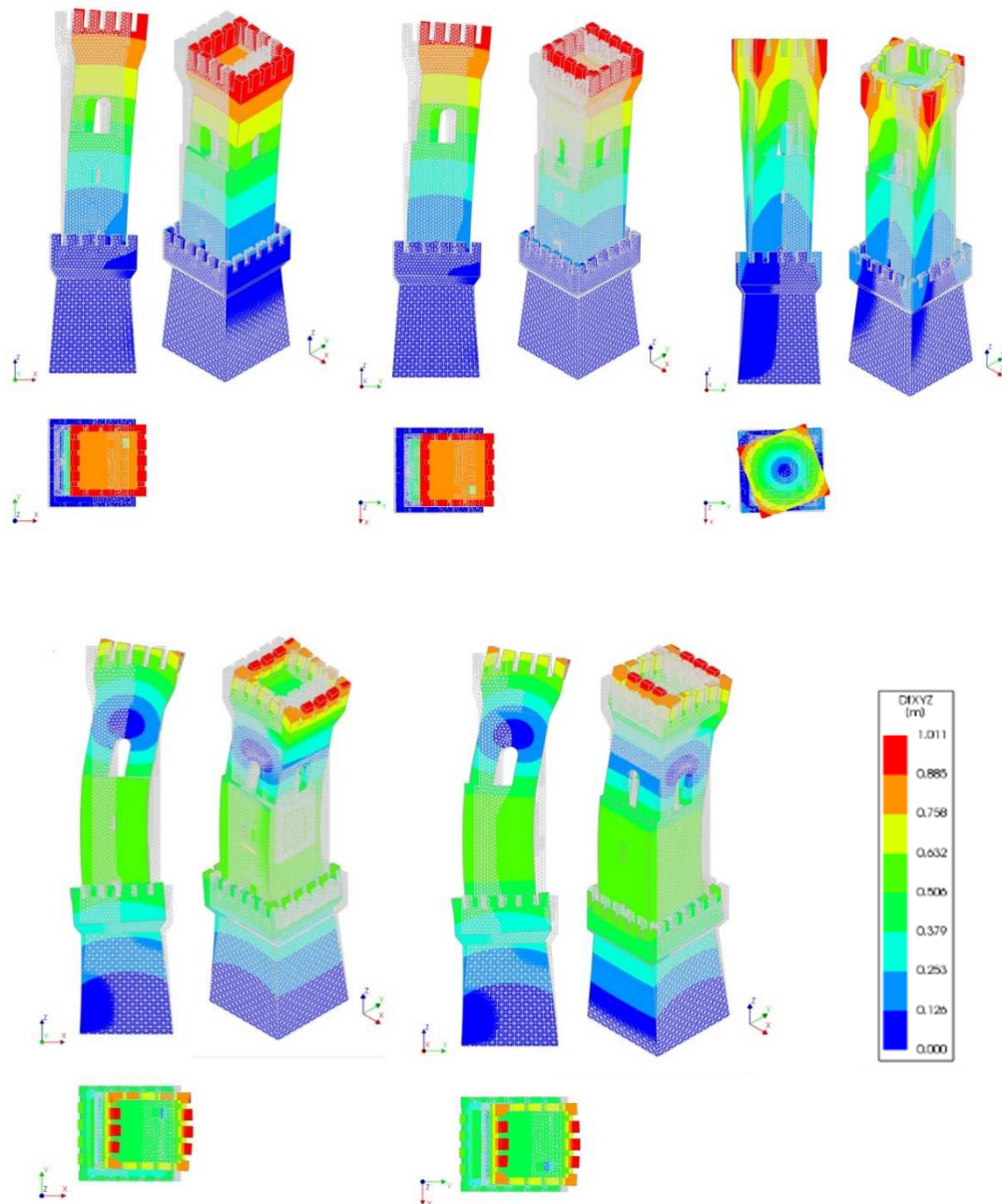


Figure 4-4 – Mode shapes of the initial model

The first and the second mode are translational respectively in X and Y; the third mode is torsional. These three mode shapes are equal to those obtained with the experimental model. In Figure 4-4 are reported the fourth and the fifth mode shape of the numerical model: the fourth is a bending mode in X-direction while the fifth is bending in Y-direction. In the experimental model the fourth mode was bending in Y-direction; this means that the fourth mode of the experimental model corresponds to the fifth mode of the numerical model. The sensors position for the monitoring campaign did not allow obtaining the actual fourth mode. It can be concluded that the fourth mode of the experimental model is therefore the fifth mode.

The results of the analysis in terms of natural frequency (Hz), period (s), effective mass percentage in X and Y directions (%), are shown in the following Table.

Mode n°	Frequency	Period	Eff. Mass	Eff. Mass	Frequency	Δf (%)
	NM	NM	X	Y	AVS	
1	1.607	0.622	33.776	0.005	2.078	22.66
2	1.632	0.613	0.005	33.804	2.152	24.16
3	5.192	0.193	0.069	0.000	6.289	17.44
4	5.973	0.167	28.13	0.000	-	-
5	6.025	0.166	0.000	28.117	6.900	12.681

Table 4-3 – Results of the analysis of the initial model

In the last column of Table 4-2 it is reported the scatter between analytical and experimental values of natural frequencies, defined as:

$$\Delta f [\%] = \left| \frac{f_i^e - f_i^a}{f_i^e} \right| 100 \quad (20)$$

where f_i^e is the experimental value and f_i^a is the analytical value of the natural frequency for the i th mode.

The frequencies of the numerical model are very low and the percent error is high. The absence of similarity makes necessary the updating procedure.

The percentages of the effective mass reflect the mode shapes. The third mode is the torsional one and its effective mass is relatively low as expected.

4.2 Modal updating procedure

The modal updating procedure consists of iteratively changing updating parameters to make the structure better match the target responses [17-19,27,28]. It is part of verification and validation of numerical models. The differences between experimental and numerical dynamic characteristics can be minimized by means of this procedure. In this way, an updated finite element model can represent current realistic behaviour of the structure.

The calibration process is based on several steps. In each step, mode shapes of the numerical model are shown and the results of the calibration are explained.

The frequencies obtained with the numerical model were lower than the experimental ones: that means that the model is not stiff enough and properties should be modified in order to obtain more accurate results. The modulus of elasticity and also the mass density were used as variables to calibrate the model.

In this process, different eigenvalue analysis were performed changing just one of these properties at each time. After calibration and optimization the final eigenfrequencies were obtained together with the recalculated values for the initial variables.

4.2.1 First step of calibration

In the first step of calibration, the material parameters are not changed and are equal to the ones of the initial model.

Material	E (MPa)	ν	γ (kN/m ³)
Masonry	1800	0.2	18
Concrete	18000	0.2	25
Filling	1100	0.2	18

Table 4-4 – Material properties of the first step of calibration

The tie-rods were added to the model. These can be identified by the command “Tyings” which assure linear dependencies between nodal variables. A tying consists of a degree of freedom in a *master* node and one or more degrees of freedom in *slave* nodes. Degrees of freedom for tyings are specified by means of a *type*: translation or rotation, and a

direction number. In this case, the translation of some nodes was fixed in X and Y direction. This can be written directly in the *dat. file*, that can be exported from Diana. An extract of it is shown in the following Figure.

```
' TYINGS '
EQUAL TR 2
14348 18957
14433 18958
14499 18304
14502 18303
14713 18451
14714 18373
EQUAL TR 1
17386 16381
241 289
17572 16538
17837 16803
17594 16566
17581 16545
17584 16556
17472 16458
```

Figure 4-5- The numbers of the first column are the masters; the numbers of the second column are the slaves. With this command, the slave nodes are forced to move in the same direction of the masters, respectively in Y and X direction

The modified *dat.file* was re-imported in Diana and an eigenvalue analysis was performed. The results of it were listed in Table 4-4 and Figure 4-6.

Mode n°	Frequency NM	Period NM	Eff. Mass X	Eff. Mass Y	Frequency AVS	Δf (%)
1	1.601	0.625	35.870	0.000	2.078	22.95
2	1.631	0.613	0.000	35.784	2.152	24.21
3	5.260	0.190	0.009	0.001	6.289	16.36
4	6.102	0.164	28.688	0.003	-	-
5	6.163	0.162	0.003	28.782	6.900	10.68

Table 4-5 – Results of the first step of calibration

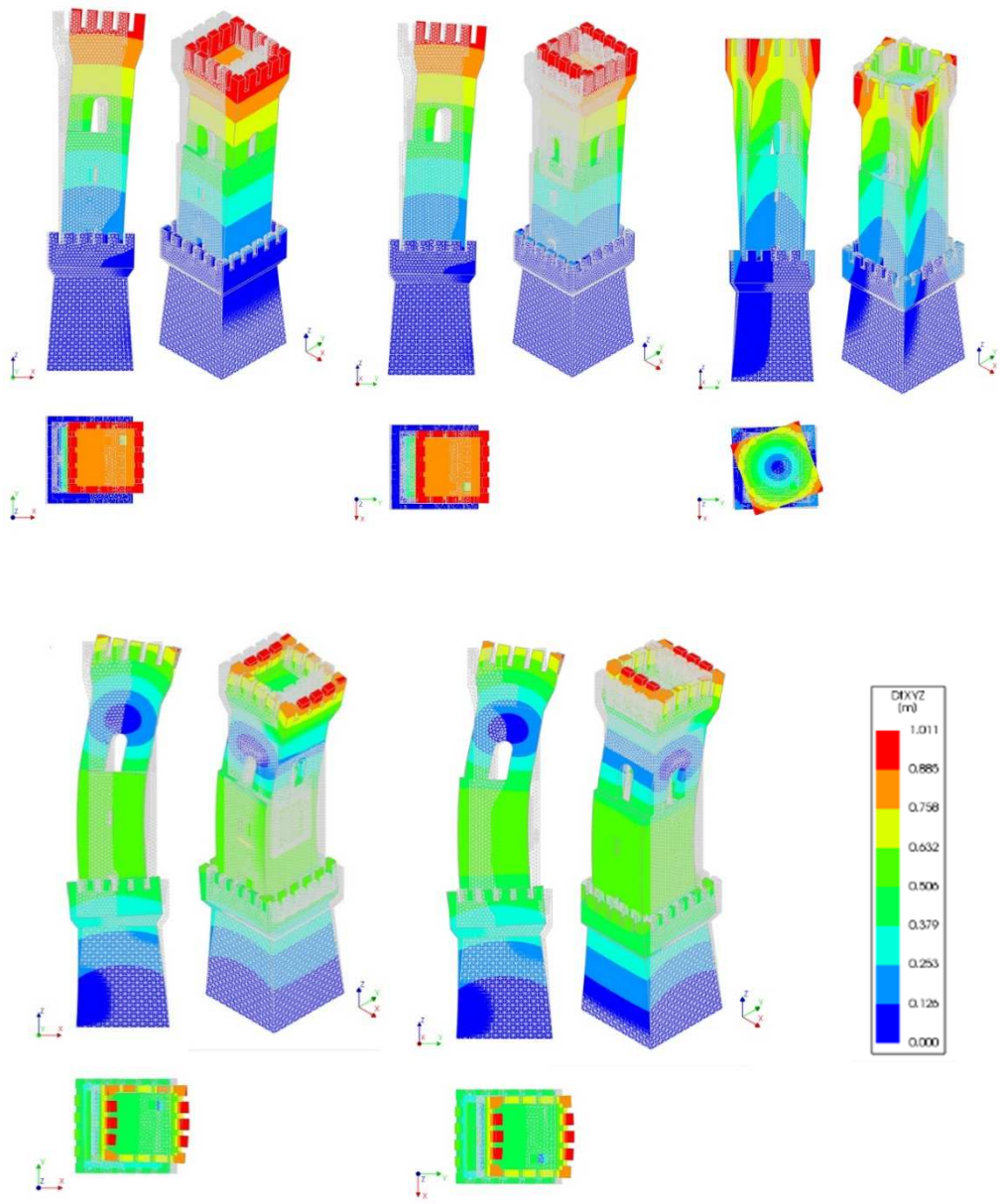


Figure 4-6 - Mode shapes of the first step of calibration

The mode shapes are correct. The natural frequencies are still low; the introduction of tie-rods did not bring much benefits and another step of calibration is necessary.

4.2.2 Second step of calibration

The second try consisted of creating another filling at the base, as shown in Figure 4-7. This derived from the idea that it is impossible that a thickness of 2.15m is entirely made of masonry bricks. The sloped external covering of the base was considered being a two-leaf masonry wall connected to the main central body of the tower by a filling.



Figure 4-7 – Mock-up of the second step of calibration. The filling is represented in purple colour, while the masonry parts are in light blue.

The modulus of elasticity of masonry and concrete was increased in order to try to conceal the discrepancy between the frequencies. The properties used for the materials were logical within the range reported in Table 4-6.

<i>Tipologia di muratura</i>	f_m	t_0	E	G
	N/cm^2	N/cm^2	MPa	MPa
muratura in mattoni pieni e malta di calce	240	6,0	1200	400
	400	9,2	1800	600
muratura in mattoni semipieni con malta cementizia	500	24	3500	875
	800	32	5600	1400
muratura in mattoni pieni e malta cementizia	780	24	8581	2537
	1537	36	16731	6971

Table 4-6 – Properties of solid brick masonry and lime mortar, brick masonry with cement mortar, solid brick masonry with cement mortar

The parameters shown in Table 4-6 were extrapolated from studies conducted on some masonry buildings [29-35]. The aim of the study was expanding Table 4-1 (Italian NTC2018): the current Italian legislation provides the values for a reduced number of building typologies and for example a masonry composed of solid bricks and cement mortar is not included in the table.

The Table 4-7 illustrates the properties assigned to materials for this second step of calibration.

Material	E (MPa)	v	γ (kN/m³)
Masonry	3000	0.2	18
Concrete	30000	0.2	25
Filling	1100	0.2	18

Table 4-7 – Material properties of the second step of calibration

The results of the eigenvalue analysis are reported in Table 4-8 and Figure 4-8.

Mode n°	Frequency NM	Period NM	Eff. Mass X	Eff. Mass Y	Frequency AVS	Δf (%)
1	1.998	0.501	36.870	0.001	2.078	3.85
2	2.043	0.489	0.001	36.730	2.152	5.06
3	6.697	0.149	0.003	0.001	6.289	6.49
4	7.575	0.132	29.150	0.003	-	-
5	7.668	0.130	0.003	29.180	6.900	11.13

Table 4-8 – Results of the second step of calibration

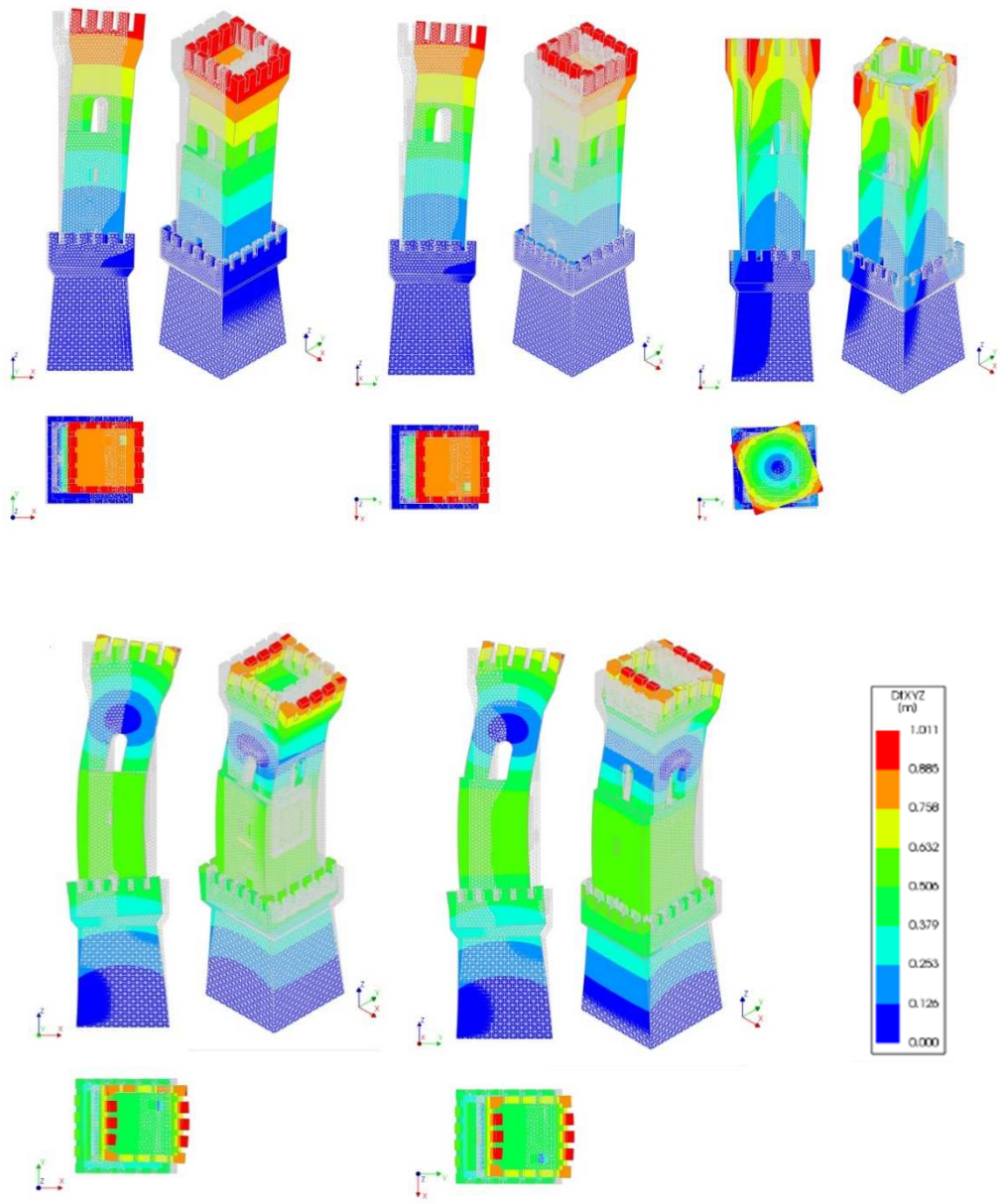


Figure 4-8 – Mode shapes of the second step of calibration

The mode shapes are equal to the experimental ones. The percent error is diminished for all the frequencies but still not acceptable. A third step of calibration is required.

4.2.3 Third step of calibration

In the third step of calibration different parameters were assigned to parts of the masonry structure. This was decided after assuming that the top of the tower and the basement were “new parts”, probably reconstructed in 1950, as can be noticed from the different tonality of colour of the façade.



Figure 4-9 – A photo of the main facade of the Civic Tower. The basement and the top of the tower, highlighted by red rectangles, were probably reconstructed in the fifties’: this is visible from the different tonality of colour of these masonry parts.

Therefore, it was necessary to create another model in FX+. The new model is composed of 15 solids and was then meshed using the same mesh size of the previous mock-up. The meshed model had 40296 points and 182400 tetrahedral elements. Figure 4-10 shows the model.

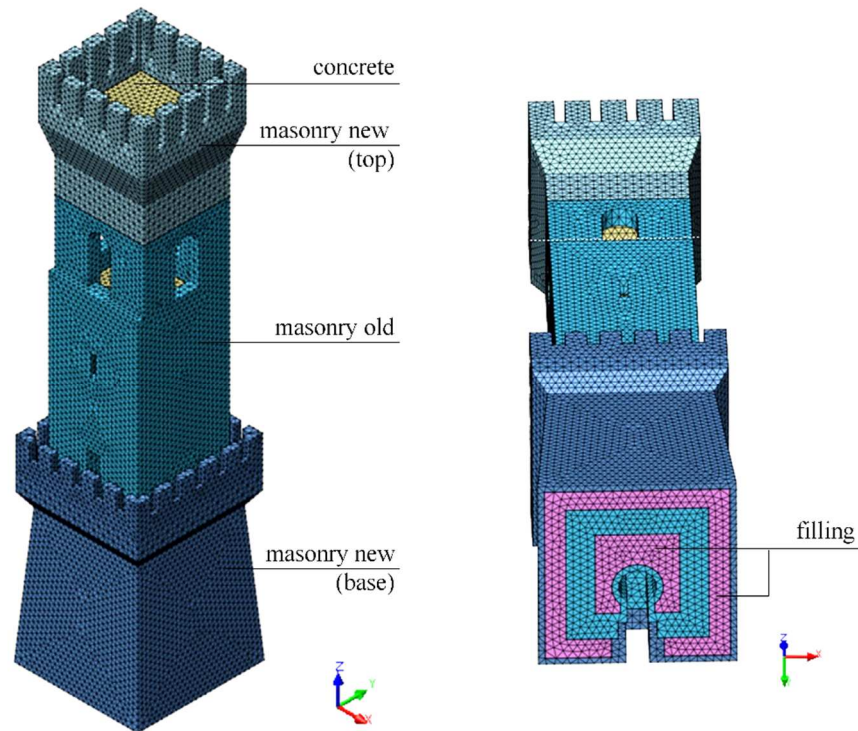


Figure 4-10 – Meshed mock-up of the third step of calibration

The new materials assigned and the respective parameters are listed in Table 4-8. The Young's modulus of “masonry new (base)” was increased to 8200 MPa: it is a quite high value but it can be accepted considering the good quality of the masonry of this part of the tower.

Material	E (MPa)	ν	γ (kN/m³)
masonry new (top)	2400	0.2	18
masonry old	2340	0.2	18
masonry new (base)	8200	0.2	18
concrete	30000	0.2	25
filling	1200	0.2	18

Table 4-9 – Material properties of the third step of calibration

The results of the eigenvalue analysis are shown in the following Table 4-10.

Mode n°	Frequency	Period	Eff. Mass	Eff. Mass	Frequency	Δf
	NM	NM	X	Y	AVS	(%)
1	2.086	0.479	32.674	0.001	2.078	0.38
2	2.133	0.469	0.001	32.182	2.152	0.88
3	6.306	0.158	0.000	0.000	6.289	0.27
4	7.736	0.129	29.490	0.002	-	-
5	7.895	0.127	0.002	30.006	6.900	14.42

Table 4-10 – Results of the third step of calibration

The first three frequencies are perfectly calibrated, the percent error is very low. The fifth is instead very high compared to the experimental one and the percent error is 14.42%. There is the need of performing another step of calibration in order to adjust the value of the fifth frequency and to obtain a percent error lower than 5% for all the fourth natural frequencies estimated.

Figure 4-11 shows that the mode shapes are again correct.

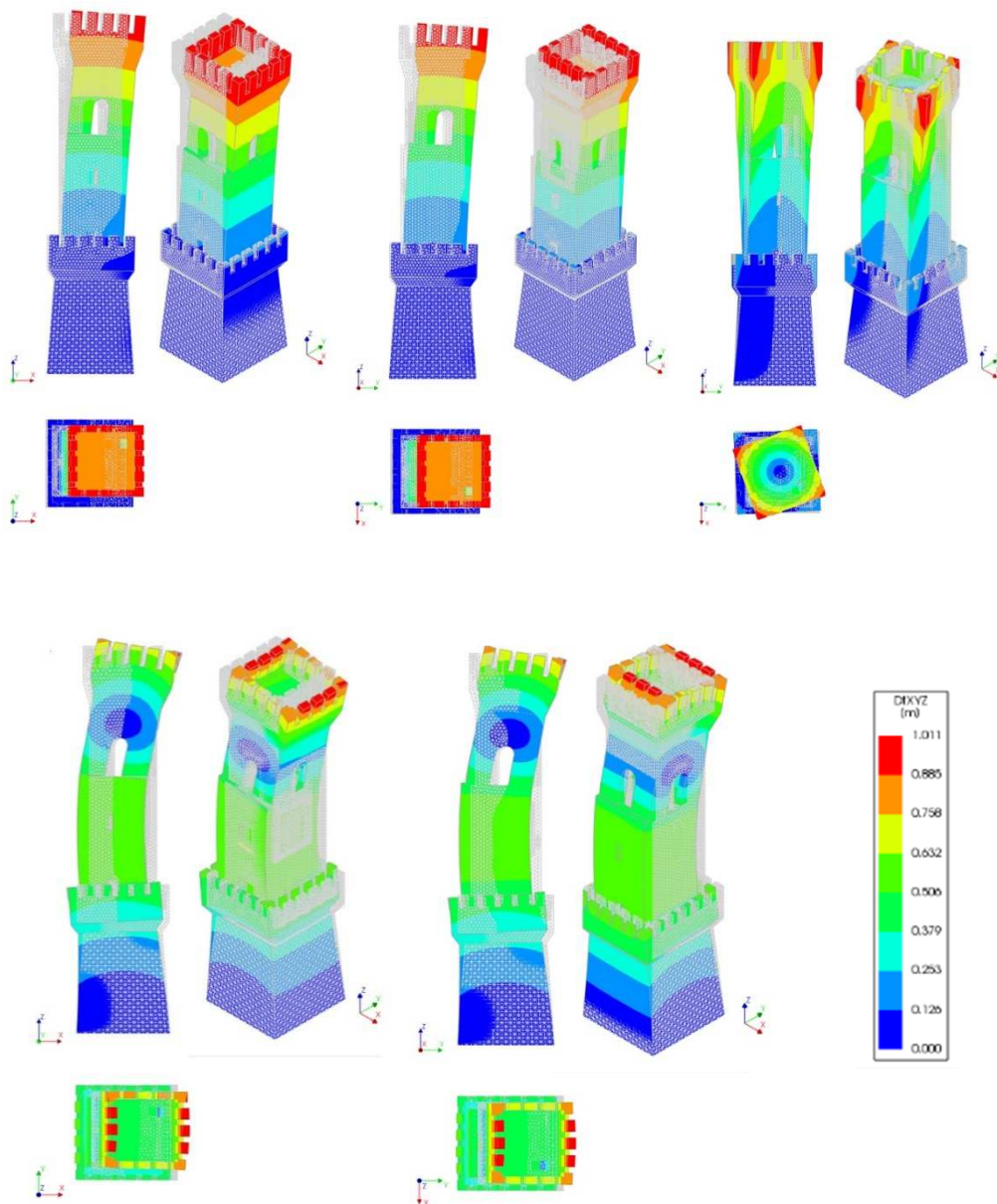


Figure 4-11 – Mode shapes of the third step of calibration

4.2.4 Sensitivity analysis

A sensitivity analysis, that is the study of how the uncertainty in the output of a mathematical model or system can be divided and allocated to different sources of uncertainty in its inputs, was carried out in order to improve the agreement observed in third step of calibration [26]. Sensitivity coefficients were calculated as

$$S_{ik} = 100 \frac{X_k}{f_i^{FEM}} \frac{\Delta f_i^{FEM}}{\Delta X_k} \quad (21)$$

X_k being the k -th uncertain parameter, f_i^{FEM} being the i -th natural frequency predicted by the numerical model and Δ being the difference operator. By adopting this definition, sensitivity coefficients represent the percentage changes in modal frequencies produced by a 100% change in parameter.

In this case, the parameter that was varied is the Young's modulus E: the elastic modulus of each material was increased by 5% one by one.

The results in terms of sensitivity coefficients are presented in Table 4-10

Mode nr	E masonry old	E masonry new (base)	E masonry new (top)	E filling	E concrete
1	16.948	22.484	0.000	0.551	13.775
2	17.213	23.288	0.527	0.790	13.175
3	7.213	2.470	0.663	0.090	3.016
5	3.707	6.796	0.500	0.346	5.287

Table 4-11 – Sensitivity coefficients for the Young's modulus of the materials

These results show that the first and the second mode are highly sensitive to the Young's modulus of "masonry old" and "masonry new (base)". It is therefore necessary to operate on these two parameters in order to better tune (calibrate) the model in terms of frequency.

4.2.5 Last step of calibration

Based on the previous sensitivity analysis, one last step of calibration have been performed. This last step of calibration aims to conceal the discrepancy between the frequencies of the fifth mode. In order to diminish this frequency, a new model of the tower was built and it was divided in 21 solids. After some attempts, twelve different materials were assigned, the parameters of those are reported in Table 4-12.

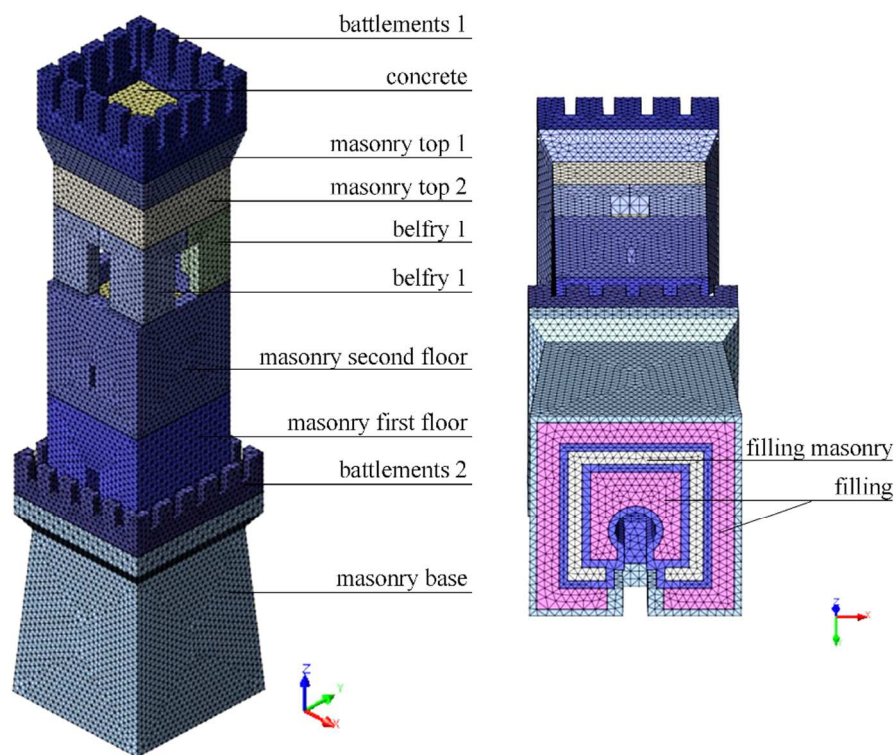


Figure 4-12 – Meshed model of the last step of calibration

The meshed model had 45342 points and 212026 tetrahedral elements.

Material	E (MPa)	ν	γ (kN/m ³)
Battlements 1	3700	0.20	18
Masonry top 1	4600	0.18	17
Masonry top 2	4500	0.20	17
Belfry 1	1000	0.17	17
Belfry 2	1100	0.17	17
Masonry second floor	3700	0.16	20
Masonry first floor	3900	0.18	21
Filling masonry	2700	0.17	19
Battlements 2	1000	0.18	21
Masonry base	4400	0.18	21
Concrete	18000	0.20	25
Filling	1100	0.20	18

Table 4-12 – Material properties of the last step of calibration

The weight of the bell and of the clock were also added to the model as masses; their values, shown in Table 4-13, were taken from the metric calculation of the restoration of the tower found in the State Archives.

	Weight
Bell	800 Kg
clock	200 Kg

Table 4-13 – Weight of the bell and of the clock inside the tower

The results of the eigenvalue analysis are illustrated in the following Table 4-14 and Figure 4-13.

Mode n°	Frequency	Period	Eff.	Eff. Mass	Frequency	Δf	MAC
	NM	NM	Mass X	Y	AVS	(%)	(%)
1	2.103	0.475	34.017	0.001	2.078	1.20	98.10
2	2.140	0.467	0.001	33.539	2.152	0.56	97.32
3	6.164	0.162	0.002	0.000	6.289	1.98	45.53
4	7.120	0.140	28.444	0.045	-	-	-
5	7.156	0.139	0.046	28.570	6.900	3.71	89.56

Table 4-14 – Results of the last step of calibration

The percent error for all the natural frequencies calculated is now lower than 5%. The properties used for the materials were logical within the range established. The conclusion is that the model is rather calibrated and it can be used for later analysis because it properly represents the behaviour of the structure. The consistency of the mode shapes was checked using the Modal Assurance Criterion (MAC) (see paragraph 4.2.5.1), whose values are reported in the last column of Table 4-14. The displacements used to measure the MAC were calculated only for the nodes where the accelerometers were put. The percentages are almost all over 80% and this again shows a good correlation between the experimental and the numerical modes so the model is properly defined. The only worrying value is the MAC of the third mode that is 45.53%, a very low percentage. This

is probably due to the predominant complexity part of the third experimental mode, as previously reported in Chapter 3.

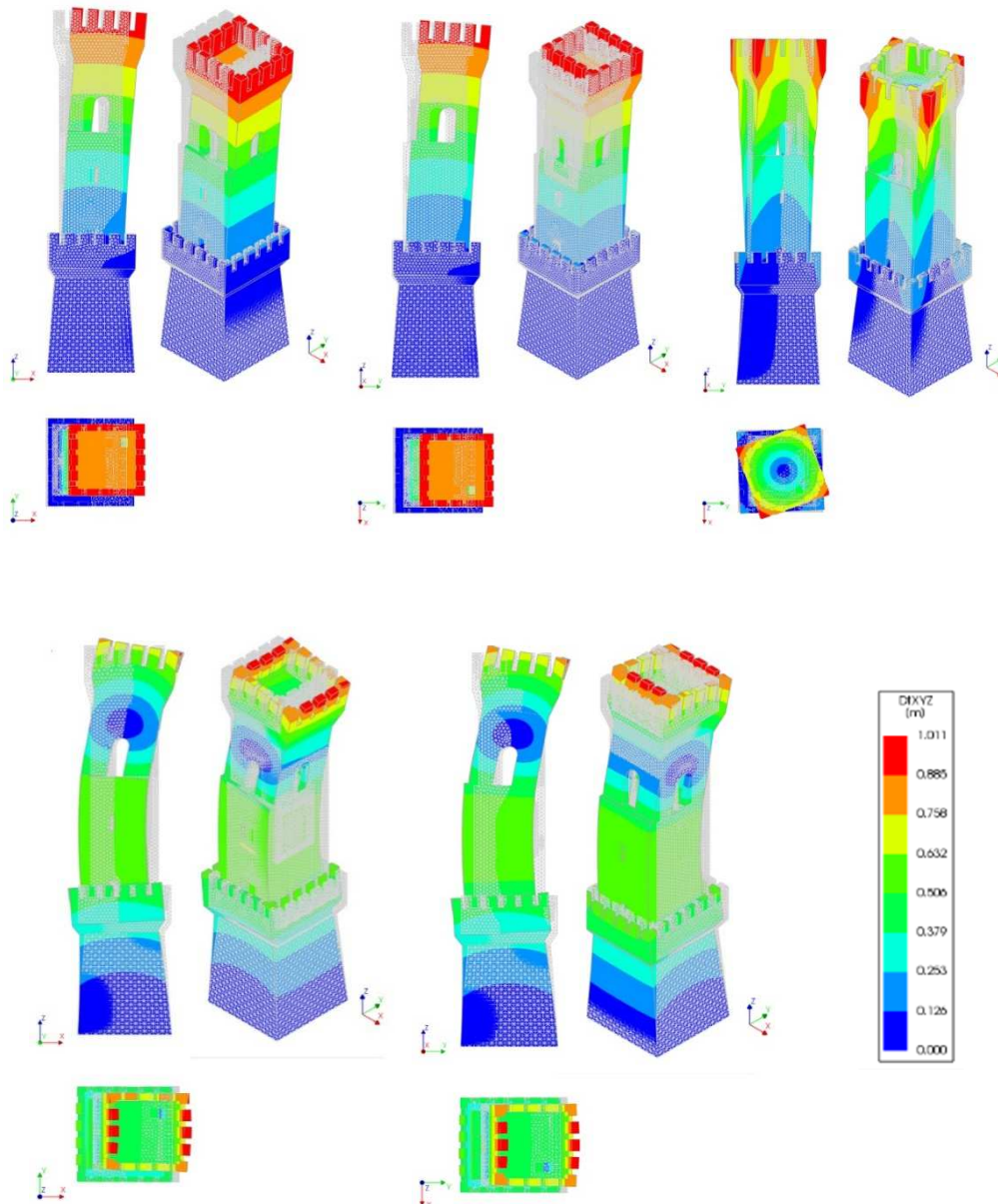


Figure 4-13 – Modal shapes of the last step of calibration

4.2.5.1 Modal Assurance Criterion (MAC)

The Modal Assurance Criterion is a statistical indicator that is most sensitive to large differences and relatively insensitive to small differences in the mode shapes [21-24]. This yields a good statistic indicator and a degree of consistency between mode shapes. The main advantages of the MAC are its straightforward implementation, as it does not

require coordinate-complete experimental eigenvectors or system matrices, and its independence of the scaling of mode shapes. It is bounded between 0 and 1, with 1 indicating fully consistent mode shapes. It can only indicate consistency and does not indicate validity or orthogonality. A value near 0 indicates that the modes are not consistent.

The MAC is calculated as the normalized scalar product of the two sets of vectors $\{\varphi_A\}$ and $\{\varphi_X\}$. The resulting scalars are arranged into the MAC matrix

$$MAC(r, q) = \frac{|\{\varphi_A\}_r^T \{\varphi_X\}_q|^2}{(\{\varphi_A\}_r^T \{\varphi_A\}_r) (\{\varphi_X\}_q^T \{\varphi_X\}_q)} \quad (22)$$

where $\{\varphi_A\}_r$ is a compatible analytical modal vector, mode r, $\{\varphi_A\}_r^T$ is the transpose of $\{\varphi_A\}_r$; $\{\varphi_X\}_q$ is test modal vector, mode q and $\{\varphi_X\}_q^T$ is the transpose of $\{\varphi_X\}_q$.

An equivalent formulation is

$$MAC(A, X) = \frac{|\sum_{j=1}^n \{\varphi_A\}_j \{\varphi_X\}_j|^2}{(\sum_{j=1}^n \{\varphi_A\}_j^2) (\sum_{j=1}^n \{\varphi_X\}_j^2)} \quad (23)$$

If a linear relationship exists (i.e., the vectors move the same way) between the two complex vectors, the MAC value will be near to one. If they are linearly independent, the MAC value will be small (near zero).

The MAC can take on value near zero for the following reasons:

- The system is non-stationary resulting from changes in the mass, stiffness and damping properties during testing
- The system is non-linear
- There is noise on the reference mode shape
- The parameter extraction technique is invalid for the measured data set
- The mode shapes are linearly independent. While the MAC is not a true orthogonality check since the mass or stiffness matrices have not been included in the calculation, it can be used as an approximation of an orthogonality check

The MAC can take on a value near unity for the following reasons:

- The number of response degrees of freedom is insufficient to distinguish between independent mode shapes

- The mode shapes are a result of unmeasured forces to the system
- The mode shapes are primarily coherent noise
- The mode shapes represent the same motion different only by a scalar

A complex vector includes both amplitude and phase, whereas a real vector is real part only. In Equation (22), it is also clear that the MAC is not sensitive to scaling, so if all mode shape components are multiplied with the same factor, the MAC will not be affected.

If an experimental modal analysis had 20 different nodes where measurements were made, the mode shape components at all 20 nodes are taken into account to calculate the MAC value, but more importance will be attributed to the higher amplitude node locations.

4.3 Calibration using Midas FEA

Midas FEA is another software for finite elements design and calculation. As Diana, it is able to perform advanced analysis for civil and structural engineering applications.

The geometrical model of the tower described in the previous paragraph was imported in Midas FEA, was meshed, and the same material properties and boundary conditions (see Table 4-11 and 4-12) were assigned.

An eigenvalue analysis was performed; the results are shown in Table 4-14 and Figure 4-13.

Mode n°	Frequency	Period	Eff. Mass	Eff. Mass	Frequency	Δf	MAC
	NM	NM	X	Y	AVS	(%)	(%)
1	2.102	0.476	34.017	0.001	2.078	1.16	98.10
2	2.140	0.467	0.001	33.539	2.152	0.56	97.32
3	6.164	0.162	0.002	0.000	6.289	1.98	45.53
4	7.118	0.140	28.444	0.045	-	-	-
5	7.153	0.139	0.046	28.570	6.900	3.67	89.56

Table 4-15 – Results of the calibration with Midas FEA

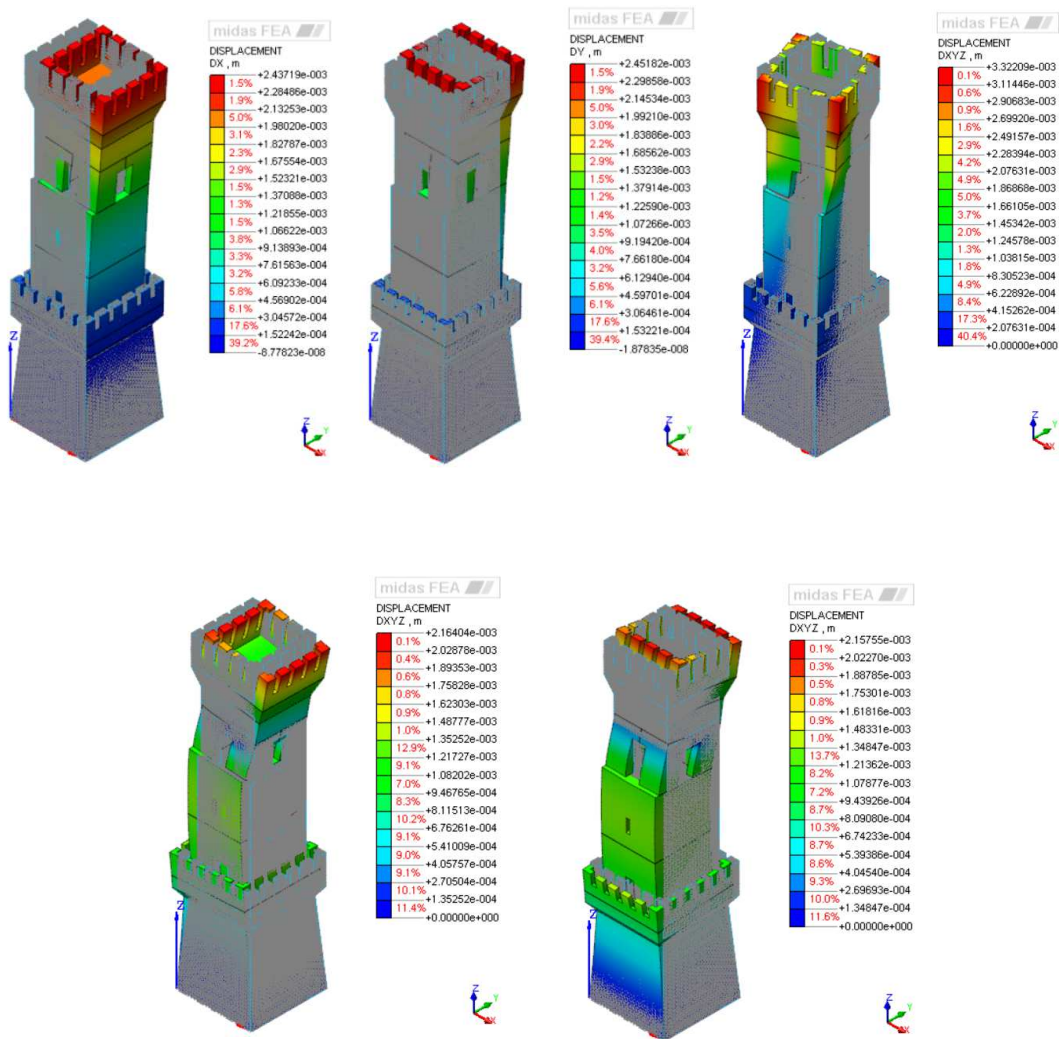


Figure 4-14 – Modal shapes of the calibration with Midas FEA

The mode shapes are identical to the ones obtained with Diana software: the first and the second mode are translational, the third is torsional and the last two are bending. The other results in terms of frequency and MAC index shown in Table 4-15 are also equal to the ones in Table 4-14

4.4 Identification of structural damage

The calibration of the numerical model brought to obtain circa the same results of the operational modal analysis with experimental data. In order to achieve the experimental frequencies, many attempts have been done on the mock-up changing iteratively the mechanical parameters of the materials. Finally, twelve different Young's moduli were assigned to likewise parts of the model, as reported in Table 4-11 . The final parameters cover a wide range of values: from very low value of the belfry to high moduli of the basement and the top. The latter are justified by assuming that those parts were restructured and built in the recent years: from the material survey, described in chapter two, it has been possible to observe that the mortar was of good quality, a cement mortar, and the solid bricks were intact.

The same can not be said for the central body of the tower, probably composed of some original seventeenth-century parts that was not destroyed after the war. Particular attention must be paid to the belfry part, where the original bell is placed. The presence of large openings, which is a common characteristic of ancient towers, make the structure vulnerable to dynamic actions, such as bell swinging or earthquakes.



Figure 4-15 – A photo of the belfry of the Civic Tower

The final elastic modulus assigned to that part is very low (1000-1100 MPa) compared to the other parameters: this means that this section is weak and the causes may be the deterioration and the poor quality of the masonry, being it the original masonry, or the

presence of local damage. Anyway, no significant and alarming cracks are visible to the naked eye. Damage detection represents the first level of damage assessment and even if it is not as precise as damage localisation and its severity evaluation, it allows to better understand the actual condition of the structure, to predict a possible future behaviour and to operate interventions in a correct way.

A linear dynamic analysis, a pushover analysis or a non-linear dynamic analysis are fundamental to detect possible collapse mechanisms.

Chapter 5

Conclusions and prospects

Ancient masonry towers represent a significant part of existing Cultural Heritage buildings, considering the high number of historic churches especially in a country like Italy. Over the centuries, many towers were built with different functions and characteristics. The necessity to preserve and maintain these strategical architectures and also to eventually plan interventions without operate destructive actions is of primary importance. Within this context, structural health monitoring is one of the most reliable non-invasive technique, which allows the prediction, and prevention of possible structural damages. However, this technique still present several limitations.

This thesis exemplifies the application of vibration-based damage detection strategy to an ancient masonry tower. In the first part of the work, great importance was given to the historical, geometrical and material survey. The available information on historic evolution, masonry inspection and on-site survey could help in the damage interpretation but also in driving further investigation. The second part discussed about the monitoring campaign and the evaluation of experimental natural frequencies. After a brief introduction to the mathematical formulation of the method, the ambient vibration testing was explained. The tower was monitored in two different periods of the year and an

operational modal analysis was performed on the data extracted. Finally, in the last chapter, it is described the procedure to calibrate the finite element numerical mock-up of the tower. The calibration of the model passed through four different steps where mechanical parameters, in particular the elastic moduli of the materials, were changed iteratively in order to fit the natural frequencies obtained with the experimental data.

The difficulty of this procedure was mainly due to the uncertainties related to the materials and the structure of the tower. In particular, the composition of the basement was not clear from the beginning and no documents or drawings regarding this part were found. Finally, a good consistency between experimental results and numerical results was obtained and the outcomes were satisfactory

Numerical model was used to predict the mechanical behaviour of the tower and may also serve as baseline condition for the implementation of a modal-based structural health monitoring (SHM). Model updating helped in the detection and localization of damage.

The results of the whole investigation suggest the following conclusions: low-cost dynamic monitoring systems, combined with state-of-art tool for Operational Modal Analysis, are effective means to provide reliable information on the evolution of the lower vibration modes of a masonry tower. Through the building of a finite element numerical model and the application of an upgrading calibration procedure, it is possible to find the realistic linear mechanical parameters of the structure analysed. Even though these parameters have some degrees of uncertainty, they are extremely helpful in the comprehension of the mechanical response of the structure to external forces and are basic information for further and more sophisticated analysis.

With regard to the detection and localization of the structural damage, the following issues are subject of future research: a linear dynamic analysis should be performed by applying the spectrum of the earthquake in the two main directions of the tower in order to evaluate possible collapse mechanisms. A pushover analysis (static non-linear analysis) with the verification of seismic actions, or a cinematic linear analysis calculating the spectral acceleration that would lead to the activation of the mechanism and the safety factor of the structure, may likewise be of great help. For an in-depth comprehension of the seismic response of the structure, a non-linear dynamic analysis should be carried out introducing non-linear parameters characteristics.

It may be concluded that dynamic measurements based on environmental vibrations, combined with appropriate model upgrading procedures, definitely represent an opportunity for the minimisation of the impact of structural evaluation on heritage structures. Further researchers may improve these procedures at the aim of preserving and protecting the great historical heritage of the world.

References

[1]-A. De Stefano et al., "Structural health monitoring of historical heritage in Italy: some relevant experiences", *J Civil Struct Health Monit* (2016).

[2]-S. Das et al., "Vibration-based damage detection techniques used for health monitoring of structures: a review", *J Civil Struct Health Monit* (2016).

[3]-A. Saisi et al., "Static and dynamic monitoring of a Cultural Heritage bell-tower in Monza, Italy", *Procedia Engineering* 199 (2017).

[4]-F. Khoshnoudian et al., "Structural damage diagnosis using modal data", *Scientia Iranica Transactions A: Civil Engineering* (2011).

[5]-A. Pierdicca et al., "Vibration-based SHM of ordinary building: detection and quantification of structural damage", DETC2015-46763. In *International Design Engineering Technical Conferences & Computers and Information in Engineering Conference - IDETC/CIE 2015*. Boston (USA), pp.1–7.

[6]-H. S. Park et al., "Damage detection of building structures under ambient excitation through the analysis of the relationship between the modal participation ratio and story stiffness", *J. of Sound and Vibration*, (2018).

[7]-A. Alvandi et al., "Assessment of vibration-based damage identification techniques", *Journal of Sound and Vibration* 292 (2006).

[8]-C.Rainieri et al., “Non-destructive characterization and dynamic identification of a modern heritage building for serviceability seismic analyses”, *NDT&E International* (2013).

[9]-A. Pierdicca et al., “Damage detection in a precast structure subjected to an earthquake: A numerical approach”, *Engineering Structures* (2016).

[10]-A. Cabboi et al., “From continuous vibration monitoring to FEM-based damage assessment: Application on a stone-masonry tower”, *Construction and Building Materials*, (2017).

[11]-C. Gentile et al., “Ambient vibration testing of historic masonry towers for structural identification and damage assessment”, *Construction and Building Materials* 21 (2007).

[12]-J.W.Park et al., “Wireless sensor network for decentralized damage detection of building structures”, *Smart Structures and Systems*, (2013).

[13]-, F. Federici, , F. Graziosi, M. Faccio, A. Colarieti, V. Gattulli, M. Lepidi and, F Potenza “An integrated approach to the design of wireless sensor networks for structural health monitoring”, *International Journal of Distributed Sensor Networks* (2012)

[14]-, F. Federici, R. Alesia , A. Colarieti M. Faccio F. Graziosi, V. Gattulli, and F Potenza , “Design of wireless sensor nodes for structural health monitoring applications”, *Procedia Engineering*,(2014)

[15]-L.F. Ramos et al., “Monitoring historical masonry structures with operational modal analysis: Two case studies”, *Mechanical Systems and Signal Processing*, (2010).

[16]-Mariella Diaferio et al., “Prediction of the fundamental frequencies and modal shapes of historic masonry towers by empirical equations based on experimental data”, *Engineering Structures*, (2018).

- [17]-F. Clementi et al., “Numerical model upgrading of a historical masonry building damaged during the 2016 Italian earthquakes: the case study of the Podesta` palace in Montelupone (Italy)”, *J Civil Struct Health Monit* (2017).
- [18]-A.Pierdicca et al.,” One-year monitoring of a reinforced concrete school building: Evolution of dynamic behavior during retrofitting works, *Procedia Engineering* (2017).
- [19]-A. Pierdicca et al., “Numerical model upgrading of a historical masonry palace monitored with a wireless sensor network”, *Int. J. Masonry Research and Innovation*, Vol. 1, No. 1, (2016).
- [20]- C. Rainieri, and, G. Fabbrocino “Operational Modal Analysis of Civil Engineering Structures”, Springer New York, New York, NY (2014)
- [21]- Maik Brehm , VolkmarZabel a, ChristianBucher “An automatic mode pairing strategy using an enhanced modal assurance criterion based on modal strain energies” *Journal of SoundandVibration*329(2010)
- [22]- Miroslav Pastora, Michal Bindaa, Tomáš Harcarika “Modal Assurance Criterion” *Procedia Engineering* 48 (2012)
- [23]- Randall J. Allemang, University of Cincinnati, Cincinnati, Ohio “The Modal Assurance Criterion – Twenty Years of Use and Abuse” *sound and vibration* (2003)
- [24]- B. J. Allemang, D. L. Drown “A correlation coefficient for modal vector analysis”
- [25]- A Borri, M Corradi, G Castori, A De Maria, “A method for the analysis and classification of historic masonry” *Bull Earthquake Eng* (2015)
- [26]- C. Gentile, F. Ubertini, N. Cavalagli, M. Guidobaldi, A.L. Materazzi, A. Saisi “Dynamic investigation of the “San Pietro” bell-tower in Perugia” *Proceedings of the 9th International Conference on Structural Dynamics, EURODYN* (2014)

[27]- H S Park , J Kim , B K Oh, “Model updating method for damage detection of building structures under ambient excitation using modal participation ratio” Measurement 133 (2019).

[28]- J N. Eiras, C Payan, S Rakotonarivo, V Garnier “Experimental modal analysis and finite element model updating for structural health monitoring of reinforced concrete radioactive waste packages” Construction and Building Materials 180 (2018).

[29]- R. Ferioli, “Muratura in zona sismica: prove sperimentali di laboratorio sulla caratterizzazione meccanica della muratura con aspetti legati alla risposta sismica di un edificio scolastico” master degree thesis 2011

[30]- C. Tambone, “Valutazione delle caratteristiche meccaniche della muratura mediante martinetto piatto doppio” master degree thesis (2015)

[31]- A Drougkas,, P Roca, C Molins “Experimental analysis and detailed micro-modeling of masonry walls subjected to in-plane shear” Engineering Failure Analysis 95 (2019)

[32]- O Bergamo, G Campione, Gaetano, E Motta, “Testing of “Global Young's Modulus E” on a rehabilitated masonry bell tower in Venice” Engineering Failure Analysis 78 (2017)

[33]- J Segura , L Pelà, P Roca, “Monotonic and cyclic testing of clay brick and lime mortar masonry in compression” Construction and Building Materials 193 (2018)

[34]- M Sy' kora , D Diamantidis, M Holicky, J Marková , Á Rózsás, “Assessment of compressive strength of historic masonry using non-destructive and destructive techniques” Construction and Building Materials 193 (2018)

[35]- A Drougka, P Roca, C Molins “Numerical prediction of the behavior, strength and elasticity of masonry in compression” Engineering Structures 90 (2015)

[36]- Á Cunha and E Caetano, “Experimental Modal Analysis of Civil Engineering Structures” University of Porto (FEUP), Portugal

[37]- S. Ivorra, F.J. Pallares, J.M. Adam, “Dynamic behaviour of a modern bell tower. A case study”, Eng. Struct. 31 (2009) 1085–1092.

Publication

M.G. Masciotta, A. Barontini, F. Clementi, F. Turchetti, S. Lenci, “Sensitivity-based versus optimization-based model updating of heritage structures: lessons learned from the application to a real case study in Ostra, Italy”, *extended abstract accepted for presentation at the Sixteenth International Conference on Civil, Structural & Environmental Engineering Computing (CIVIL-COMP), 16-19 September 2019, Riva del Garda, Italy.*

Affiliations: ISISE, University of Minho, Department of Civil Engineering, Guimaraes, Portugal; Polytechnic University of Marche, Dep. of Civil and Building Engineering, and Architecture, Ancona, Italy

